

DOI:10.16788/j.hddz.32-1865/P.2024.01.003

引用格式:王志强,周美娟,黎训飞,等.高硅花岗岩流体出溶作用的识别和意义[J].华东地质,2024,45(1):26-48.(WANG Z Q, ZHOU M J, LI X F, et al. Identification and significance of fluid exsolution in high silica granite[J]. East China Geology, 2024, 45(1):26-48.)

# 高硅花岗岩流体出溶作用的识别和意义

王志强<sup>1,2</sup>,周美娟<sup>1,2</sup>,黎训飞<sup>1,2</sup>,笪昊翔<sup>1,2</sup>

(1.合肥工业大学资源与环境工程学院矿床成因与勘查技术研究中心,安徽 合肥 230009;

2.安徽省矿产资源与矿山环境工程技术研究中心,安徽 合肥 230009)

**摘要:**高硅花岗岩以暗色矿物含量低,富SiO<sub>2</sub>、Rb,贫MgO、FeO、Sr、Ba为特征,富集稀有金属元素,其研究对于理解花岗岩成因演化、稀有金属元素富集和成矿过程至关重要。岩相学和地球化学特征指示其经历高程度的分异演化,H<sub>2</sub>O等挥发分作为不相容组分在残余熔体中逐渐富集饱和,导致流体出溶在高硅花岗质熔体中,但如何识别这一过程是难点。文章从岩相学、地球化学、矿物学、金属稳定同位素(Li、Ba、Fe)等角度总结了高硅花岗岩中流体出溶作用的证据和指标。岩相学方面,晶洞构造、雪球结构、单向固结结构等特殊结构、构造的出现是流体出溶的重要标志;地球化学方面,极低的Nb/Ta值(<5)、Zr/Hf值、稀土元素四分组效应是流体-熔体相互作用的有效识别标志;矿物学方面,锆石脱晶化作用、轻稀土元素富集及钾长石富Pb指示存在热液流体参与;金属稳定同位素方面,相对于普通花岗岩,高硅花岗岩通常富集重Li、轻Ba和重Fe同位素,流体-熔体相互作用很可能是主要控制因素。但部分地球化学指标还存在较大争论,在实际使用过程中需结合不同指标进行综合分析。经过岩浆演化和流体出溶两阶段的富集过程,稀有金属元素得以在出溶流体中极度富集进而成矿。

**关键词:**高硅花岗岩;流体出溶;岩浆-热液过渡;金属稳定同位素;稀有金属成矿

中图分类号:P581

文献标识码:A

文章编号:2096-1871(2024)01-026-23

花岗岩是地球大陆地壳的重要组成部分,是地球区别于太阳系其他行星的重要标志<sup>[1]</sup>。高硅花岗岩(SiO<sub>2</sub>>74%<sup>[2-3]</sup>)是一类特殊的花岗岩,以高硅、富碱、富集稀有金属元素为特征,与稀有金属成矿作用关系密切,其形成机制对于理解花岗质熔体在地壳浅部的运移、储存、分异演化及成矿效应具有重要意义,是目前国际上岩石学和矿床学等领域研究的热点<sup>[4-8]</sup>。花岗质熔体富含H<sub>2</sub>O、CO<sub>2</sub>、F和Cl等挥发分,这些挥发分在岩浆演化过程中为不相容组分,其含量随着岩浆演化程度的增加而显著升高。当挥发分含量超过溶解度时即发生挥发分饱和,进而形成独立挥发相<sup>[9-11]</sup>。因此,花岗质熔体从岩浆向热液演化普遍经历3个阶段:岩浆阶段

(单一熔体)、岩浆-热液过渡阶段(熔体+热液流体)和热液阶段(热液流体)<sup>[12]</sup>。岩浆-热液过渡阶段发生的流体出溶是流体从岩浆中提取成矿元素的重要过程,是成矿元素富集迁移的关键<sup>[13]</sup>。

近年来,已陆续发表了一系列关于高硅花岗岩成因的综述论文<sup>[7-8,12,14-18]</sup>,系统论述了高硅花岗岩的地质特征、地球化学特征、高度分异机制以及与稀有金属成矿关系等方面的研究进展。但这些文献多聚焦于岩浆阶段的讨论,对成矿起关键作用的岩浆-热液阶段的探讨则相对较少。一些岩相学证据(如晶洞构造、单向固结结构)<sup>[16,19]</sup>无可置疑地表明流体出溶过程的存在,但这些特殊的结构和构造并非一直出现,流体出溶过程更多地以隐秘的方式

\* 收稿日期:2024-01-15 修订日期:2024-03-07 责任编辑:谭桂丽

基金项目:国家自然科学基金“南岭燕山期骑田岭复式岩体钨、锡成矿差异机制研究(编号:41602051)”和中央高校基本科研业务费专项资金“南岭燕山期高硅花岗岩精细矿物学和Li同位素研究(编号:JZ2021HGTB0108)”项目联合资助。

第一作者简介:王志强,1987年生,男,副教授,博士,主要从事高硅花岗岩和伟晶岩成因及相关稀有金属成矿等研究工作。Email:wangzq@hfut.edu.cn。

进行, 在结构和构造上可能与普通花岗岩 ( $\text{SiO}_2 < 74\%$ ) 并无明显差别。因此, 如何识别高硅花岗岩中的流体出溶作用是研究中的难点, 一些指标也存在很大争论。本文重点关注高硅花岗岩中的流体出溶作用, 从岩相学、地球化学、矿物学和同位素(尤其是金属稳定同位素) 地球化学的角度, 总结流体出溶作用存在的证据, 为理解高硅花岗岩稀有金属元素富集和成矿过程提供参考。

## 1 高硅花岗岩基本特征

高硅花岗岩包括前人研究中常出现的高分异花岗岩、白岗岩、淡色花岗岩、 $\text{Li}-\text{F}$  花岗岩、黄玉花岗岩及翁岗岩等。高硅花岗岩和普通花岗岩主要特征对比见表 1。岩相学上, 高硅花岗岩暗色矿物

含量较低, 主要暗色矿物为黑云母, 或不含暗色矿物, 手标本下为灰白色或白色(图 1), 常见岩性有黑云母花岗岩、二云母花岗岩和白云母花岗岩。不同于普通花岗岩, 淡色花岗岩常出现一些特殊的副矿物, 如石榴石、电气石、黄玉、萤石、钛石和磷钇矿等(图 1), 有时也会出现锡石、黑钨矿、铌钽铁矿及氟碳铈矿等副矿物<sup>[7-8]</sup>。在矿物成分上, 高硅花岗岩中的黑云母一般具有富 Fe 贫 Mg 特征( $\text{Fe}/(\text{Fe}+\text{Mg}) > 0.6$ ), 接近铁黑云母端元<sup>[20-21]</sup>。白云母通常具有富锂特征, 成分为富锂白云母-锂白云母-铁锂云母-锂云母系列<sup>[22-25]</sup>。斜长石具有富 Na 贫 Ca 特征, 为中长石-钠长石系列, 一些极端演化的高硅花岗岩中斜长石几乎全部为钠长石, 形成特殊的钠长花岗岩<sup>[26-28]</sup>。

表 1 高硅花岗岩和普通花岗岩特征对比

Table 1 Comparison of characteristics between high silica granite and common granite

| 特征     | 高硅花岗岩  | 普通花岗岩  |
|--------|--|--|
| 岩石类型   | 正长花岗岩、碱长花岗岩  | 花岗闪长岩、二长花岗岩  |
| 产状     | 岩株、岩脉、小岩体  | 大岩基、岩株、岩脉、小岩体  |
| 颜色     | 白色、灰白色   | 灰白色、灰色   |
| 暗色矿物含量 | <5%  | 5%~15%   |
| 主要矿物   | 钾长石、钠长石-更长石、石英、白云母-黑云母   | 更长石-中长石、钾长石、石英、角闪石、黑云母   |
| 副矿物    | 锆石、磷灰石、独居石、石榴石、电气石、磷钇矿、富 Li-Cs-Rb 云母、氟碳铈矿、铌钽铁矿、绿柱石、钛石、黑钨矿等                                       | 锆石、榍石、褐帘石、磷灰石  |
| 矿物成分   | 黑云母富 Fe 贫 Mg; 斜长石富 Na; 锆石普遍发生脱晶作用, 富 U、LREE、Hf   | 黑云母相对富 Mg; 斜长石相对富 Ca; 锆石震荡环带发育, 贫 U、LREE、Hf  |
| 主量元素   | 高 Si, 贫 Ca、Mg、Fe、Ti、P  | 低 Si, 高 Ca、Mg、Fe、Ti、P  |
| 微量元素   | 富集 Rb、Li、Be、Cs、Nb、Ta、W、Sn、U 等不相容元素; 亏损 Ba、Sr、Zr、Ni、Co、Cr 等相容元素; 高 Rb/Sr、Rb/Ba 值, 低 Nb/Ta、Zr/Hf 值 | 亏损 Rb、Li、Be、Cs、Nb、Ta、W、Sn、U 等不相容元素; 富集 Ba、Sr、Zr、Ni、Co、Cr 等相容元素; 低 Rb/Sr、Rb/Ba 值, 高 Nb/Ta、Zr/Hf 值 |
| 稀土元素   | ΣREE 低, 平坦式稀土配分模式, 强负 Eu 异常  | ΣREE 高, 右倾式稀土配分模式, 无-中等负 Eu 异常   |

除了特殊的矿物组成外, 地球化学特征是高硅花岗岩区别于普通花岗岩更有效的指标。由于大量暗色矿物、铁氧化物、斜长石以及各类副矿物的结晶分异, 高硅花岗岩的  $\text{FeO}$ 、 $\text{MgO}$ 、 $\text{CaO}$ 、 $\text{TiO}_2$  和  $\text{P}_2\text{O}_5$  含量极低, 碱 (Na、K) 含量较高, 但  $\text{K}_2\text{O}/\text{Na}_2\text{O}$  值变化较大。在微量元素上, 高硅花岗岩的 Cr、Ni、Co、Sr、Ba 含量极低, Li、Rb、Cs、Nb、Ta、Pb 含量较高<sup>[20,29-30]</sup>, 稀有金属元素的富集使其具有极大的稀有金属成矿潜力<sup>[7,8,31-32]</sup>。由于具有高 Rb 和低 Sr、Ba 含量的特点, 高硅花岗岩具有极高的 Rb/Sr 值和 Rb/Ba 值(可达几十甚至上百)<sup>[33]</sup>。元素在岩浆中的行为主要受控于离子半径和电荷数

(CHARAC 行为), 对于离子半径和电荷相近的元素对(如 K-Rb、Nb-Ta、Zr-Hf、Y-Ho), 其比值在一个较小的范围内变化<sup>[34]</sup>。不同于普通花岗岩, 高硅花岗岩表现出异常低的 Nb/Ta、Zr/Hf、K/Rb 值以及异常高的 Y/Ho 值, 明显偏离正常岩浆岩范围而表现出 non-CHARAC 行为<sup>[35-38]</sup>。BALLOUARD C 等<sup>[39]</sup>系统总结了不同成矿类型花岗岩的 Nb/Ta 值, 发现高硅花岗岩普遍具有较低的 Nb/Ta 值, 并提出  $\text{Nb}/\text{Ta} < 5$  可以作为区分稀有金属成矿花岗岩和不成矿花岗岩的指标。此外, 由于富含稀土元素的矿物的结晶分异(如榍石、独居石、褐帘石、锆石等), 高硅花岗岩整体上表现为平坦海鸥式的稀土



(a).南岭天门山岩体,局部发育红色石榴石;(b).南岭骑田岭岩体,局部发育黑色电气石团块

图1 高硅花岗岩手标本照片

Fig. 1 Photographs of the high silica granite

元素配分模式,并显示出强的负Eu异常。而普通花岗岩一般为富集轻稀土的右倾式稀土元素配分模式,弱Eu负异常或没有Eu异常<sup>[20,30]</sup>。高硅花岗岩还常表现出特殊的稀土元素四分组效应,如南岭的姑婆山<sup>[20]</sup>、千里山<sup>[30]</sup>、西华山<sup>[40]</sup>,江南造山带的曾家垅<sup>[38]</sup>、茅公洞<sup>[41]</sup>,东北地区的卧都河岩体<sup>[36]</sup>等。

## 2 高硅花岗岩的形成机制

目前,关于高硅花岗岩的形成存在两种端元模式:地壳低程度部分熔融和花岗质熔体高度分异演化。低程度部分熔融模式认为高硅花岗岩来源于变泥质岩的部分熔融,其成分变化受控于源岩成分和部分熔融条件的变化,该模式常用于解释造山带出露的淡色花岗岩的成因,例如喜马拉雅淡色花岗岩<sup>[42-44]</sup>。高度分异演化模式认为早期结晶矿物的高度分离是残余熔体富硅、富稀有金属元素的关键。该模式的典型代表区域是南岭地区,该地区燕山期花岗岩多以复式岩体形式产出,复式岩体各期次岩体具有相近的侵位年龄及相似的Sr-Nd同位素组成,岩相学和地球化学特征具有明显的演化关系,指示同源岩浆演化关系<sup>[8,45-47]</sup>。

由于花岗质岩浆黏度大,结晶的矿物与岩浆的密度相似,部分学者认为花岗质岩浆不能或仅能发生有限的结晶分异作用<sup>[48-49]</sup>。然而近些年来,不同学者通过岩相学<sup>[50-51]</sup>、地球化学模拟计算<sup>[29,50,52]</sup>、相平衡模拟计算<sup>[53]</sup>和黏度模型<sup>[4]</sup>、热扩散模型<sup>[54]</sup>等手段进行研究,结果均表明中酸性岩浆可以发生有效的结晶分异作用,进而提出晶粥模型(mush

model)<sup>[4,55]</sup>。该模型指花岗质岩浆在岩浆房中以晶体和熔体的混合物形成存在,由于具有较高的晶体含量,岩浆流动性变弱。当晶粥中的晶体含量为50%~70%(体积分数)时,岩浆房中岩浆对流作用停止而粒间又有足够的空隙,此阶段最有利于粒间高硅熔体的抽离<sup>[4,56]</sup>。粒间高硅熔体抽离的最终产物为喷发的高硅流纹岩或浅成侵位的高硅花岗岩<sup>[57]</sup>,而岩浆房中堆积的晶体以及粒间残余的熔体形成富含斑晶的花岗质岩基。学者们提出的中酸性岩浆房中晶体-熔体分离机制主要有微沉降(micro-settling)、受阻沉降(hindered settling)、压实作用(compaction)<sup>[4,29]</sup>。而 HOLNESS M B<sup>[58]</sup>通过中酸性岩的显微结构研究认为这三种方式可能并非主要机制,指出气体压滤作用(gas filter-pressing)和外部应力(external stress)可能对熔体的抽离起到关键作用。气体压滤作用是指挥发分从粒间熔体出溶,驱动粒间熔体在晶粥中迁移<sup>[59-60]</sup>,有助于高硅熔体从晶粥体中分离。岩浆中高的H<sub>2</sub>O及其挥发分含量,以及侵位于地壳浅部等特点,均有助于挥发分的出溶和气体压滤作用发生<sup>[58]</sup>。外部应力对粒间熔体分离所起的作用也较早被学者关注,最早应用于对地壳熔融作用的研究,将区域构造、混合岩和花岗岩侵位建立起联系<sup>[61-62]</sup>。外部应力模式得到一些学者的研究支持,认为外部应力可以促进粒间高硅熔体从晶粥中抽离<sup>[63-65]</sup>。类似地,LIU X C等<sup>[66]</sup>研究认为,藏南拆离系的剪切作用有助于低黏度且富H<sub>2</sub>O、富Li的熔体从母岩浆中抽离,形成富Li伟晶岩(高硅花岗质岩石)。

### 3 高硅花岗岩中热液流体作用的识别

全岩地球化学和矿物地球化学研究表明,高硅花岗岩的形成需要高程度的分离结晶<sup>[67-68]</sup>。HAL-LIDAY A N 等<sup>[33]</sup>研究表明,全岩 Rb/Sr 值>10 的高硅花岗岩的形成需要经过 90% 以上的分离结晶;王汝成等<sup>[32]</sup>认为,Be 矿化发生需要岩浆经过 99% 的分离结晶或多阶段高程度分异演化。岩石学和数值模拟表明,花岗质岩浆发生分离结晶主要以晶体-熔体抽离作用为主。当熔体结晶 50%~70% 时熔体最容易从岩浆房中抽离;当熔体结晶>70% 时,由于粒间熔体不能连通而不易发生晶体-熔体分离<sup>[55,69]</sup>。因此,仅用岩浆演化似乎难以解释高硅花岗岩的地球化学特征。另一方面,由于 H<sub>2</sub>O 在花岗质熔体中为不相容组分,经历长时间的演化不可避免将引起流体的饱和<sup>[10,70]</sup>。而富集金属元素的出溶流体(如 W、Sn、Li、Nb、Ta)被认为是形成相关稀有金属矿床的关键<sup>[7,13,31,71]</sup>。越来越多的学者认识到,高硅花岗岩的形成不仅是分离结晶的结果,热液过程同样是高硅花岗岩成因研究中不可忽略的重要因素<sup>[30,34,38,72-73]</sup>。由于出溶的流体相大部分会随岩浆冷却而释放到体系之外,因此岩浆-热液过程难以示踪<sup>[74]</sup>。如何有效识别流体出溶以及流体在高硅花岗岩形成中的作用,已成为近年来国内外学者关注的焦点科学问题<sup>[8,25,39,73,75]</sup>。

#### 3.1 岩相学特征

花岗岩最常见的是块状构造,但一些特殊的构造具有重要的成因指示意义。晶洞是侵入岩中近于圆形或不规则的原生孔洞,在晶洞中常发育晶形完好的晶体,如石英、长石、云母,以及电气石、绿柱石、黄玉、萤石、绿帘石等矿物(图 2)。晶洞是岩浆冷凝过程中,大量挥发分向低压方向运移并逸出后形成的,因而被认为是岩浆发生挥发分出溶最好的证据<sup>[19,74,76-77]</sup>。晶洞中结晶晶体的缺乏指示孔洞中不存在硅酸盐熔体,主要为热液流体占据空间,晶体只在熔体和挥发分界面附近成核并生长<sup>[19]</sup>。晶洞一般仅出现在浅成花岗岩中,尤其是细粒花岗岩中。这是由于晶洞的形成需要岩浆在上侵减压过程中发生气泡的生长,挥发分的出溶导致固相线温度升高,岩浆因冷却而发生快速结晶,形成具有晶洞构造的细粒花岗岩、花岗斑岩和细晶岩<sup>[78-79]</sup>。晶洞随着压力的增加而减少,在压力超过 3 kbar 时一

般不发育晶洞<sup>[19]</sup>。我国浙闽沿海地区发育一条长约 800 km、宽 60~80 km 的 NE 向白垩纪晶洞花岗岩带,这些晶洞花岗岩的侵位深度也被认为<3 km<sup>[80-81]</sup>。南岭地区花岗岩晚期细粒黑云母/二云母花岗岩中也普遍发育晶洞构造,如花山岩体<sup>[82]</sup>、骑田岭岩体<sup>[8]</sup>、九嶷山岩体<sup>[83]</sup>;江南造山带也是如此,如三清山岩体、伏岭岩体<sup>[84]</sup>、元宝山岩体<sup>[85]</sup>、朱溪细粒花岗岩<sup>[86]</sup>。细晶岩、细粒花岗岩的细粒结构可能是高硅熔体中流体出溶释放,熔体固相线温度升高,熔体在过冷却状态下发生快速结晶而形成的<sup>[87]</sup>。

除了晶洞构造外,高硅花岗岩中也常发育雪球结构,如德国 Erzgerbirge、华南宜春和大吉山、大兴安岭维拉斯托等稀有金属矿床中的成矿岩体<sup>[88-91]</sup>。雪球结构为板条状钠长石晶体呈环带状出现在石英或钾长石斑晶中(图 2)<sup>[90,92]</sup>。关于雪球结构的成因,目前还存在争论,主要有岩浆成因和岩浆-热液成因两种观点。李福春等<sup>[90]</sup>通过结构和成分特征研究,指出雪球结构为岩浆成因,是岩浆中 F、Na、Al、H<sub>2</sub>O 成分变化引起晶体成核速率和生长速率发生变化的结果。然而, MÜLLER<sup>[88]</sup>对德国 Erzgerbirge 花岗岩的研究表明,雪球结构形成于温度<600°C 的条件,雪球石英同时具有岩浆石英和热液石英的阴极发光特征,指出雪球结构是富 F-Li 花岗质熔体发生流体饱和时形成的结构,同时也是稀有金属成矿岩体的指示标志。WU M Q 等<sup>[93]</sup>通过矿物结构与成分分析,指出宜春花岗岩中的雪球石英为热液流体交代成因。WANG D Z 等<sup>[94]</sup>在冀北东坪花岗斑岩的雪球石英中发现低盐度流体包裹体、高盐度流体包裹体和熔体包裹体共存,认为该现象反映了雪球石英形成于富流体熔体的岩浆-热液转换阶段。杨飞等<sup>[91]</sup>在维拉斯托稀有金属花岗岩的雪球石英中发现了共存的熔体包裹体和流体包裹体,为雪球结构的岩浆-热液成因提供了有力的证据。

另外一种指示挥发分出溶的典型结构为单向固结结构(UST, Unidirectional Solidification Texture),在与成矿相关的花岗斑岩体<sup>[95-98]</sup>、伟晶岩<sup>[99]</sup>中常见。单向固结结构指侵入体结晶过程中产生矿物、结构及组分分层,矿物晶体垂直于层走向或与层走向成高角度生长的现象,通常为石英、碱性长石或石英-碱性长石共生层的互层<sup>[16,97]</sup>(图 3)。UST 结构中的石英层被认为是从初始出溶的岩浆流体中结晶,因此指示了岩浆-热液过程及其相关成矿作用<sup>[19,100-101]</sup>。

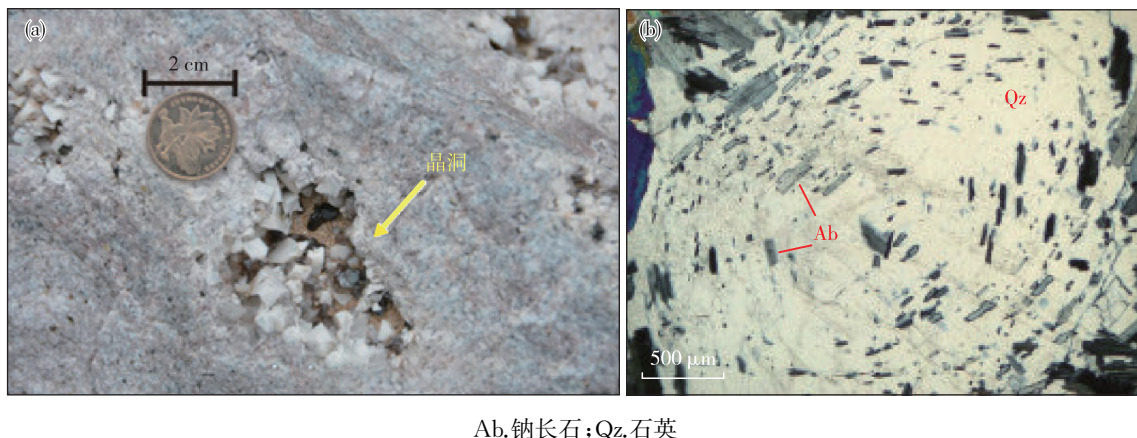


图 2 高硅花岗岩中的晶洞构造(a)<sup>[95]</sup>和雪球结构(b)<sup>[96]</sup>  
Fig. 2 Miarolitic structure (a)<sup>[95]</sup> and snowball texture (b)<sup>[96]</sup> in the high silica granite

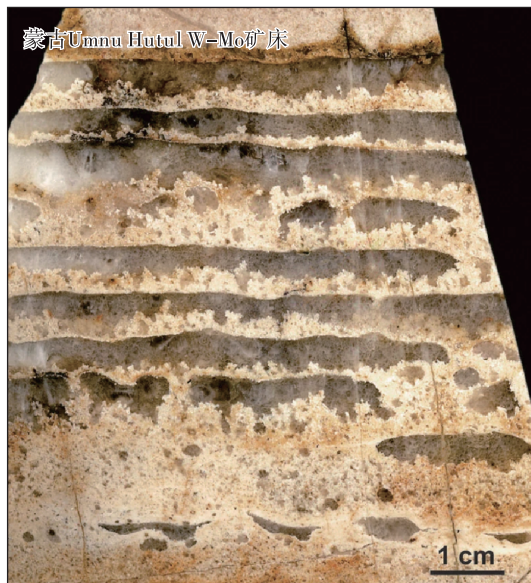


图 3 花岗岩中的单向固结结构<sup>[101]</sup>  
Fig. 3 UST texture in the granite<sup>[101]</sup>

### 3.2 全岩地球化学特征

尽管高硅花岗岩中常出现晶洞构造、雪球结构等指示流体出溶的结构构造,但也仅限于高硅花岗岩体的局部位置,流体出溶作用更多通过隐秘方式进行,如何有效识别仍是研究难点。高硅花岗岩常表现出异常的地球化学行为,如异常低的 Nb/Ta 值以及稀土元素的四分组效应等,这些特征被认为是岩体经历流体-熔体相互作用的结果<sup>[34,72]</sup>。稀土元素的四分组效应最早由 PEPPARD D F 等<sup>[102]</sup>在实验室液-液化学萃取过程中发现,指在球粒陨石标准化的配分模式图中,将 15 个镧系元素分成四组:La

到 Nd、Pm 到 Gd、Gd 到 Ho、Er 到 Lu, 分界点对应于 4f 电子层分别充填 1/4、1/2、3/4, 每组都呈现平滑的上凹或下凸形式(图 4)。目前,已在自然界海水、生物碎屑灰岩、热液成因铀矿物、稀土矿物、地下水以及稀有金属花岗岩中发现稀土元素的四分组效应<sup>[103-108]</sup>。

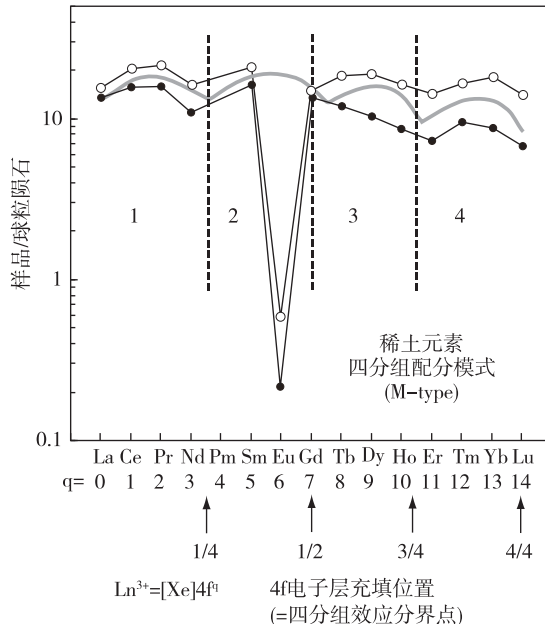


图 4 稀土四分组效应(据文献<sup>[36]</sup>修改,球粒陨石标准化值引自文献<sup>[109]</sup>)  
Fig. 4 REE tetrad effect (modified from reference<sup>[36]</sup>, chondrite normalization values are from reference<sup>[109]</sup>)

由于稀土元素四分组效应通常见于高硅花岗岩和伟晶岩中,因此一种观点认为早期矿物的分离

结晶(磷灰石、独居石、磷钇矿、石榴石)可以导致熔体四分组效应<sup>[110-112]</sup>。但 BAU M<sup>[34]</sup> 和 IRBER W<sup>[72]</sup> 的模拟计算表明,矿物分离结晶不能使熔体形成典型的四分组效应,并且这些矿物的分离结晶也不能解释与四分组效应明显相关的 Y/Ho 值和 Zr/Hf 值的变化,因此提出四分组效应是熔体与富 F 流体相互作用形成的。赵振华等<sup>[113]</sup> 对南岭千里山岩体和内蒙古巴尔哲花岗岩的系统分析发现,它们的全岩、主要造岩矿物及副矿物普遍具有稀土元素四分组效应,由此提出四分组效应并不是由某一种稀土副矿物引起的,而是岩浆高度分异最终形成的出溶流体与共存熔体相互作用的结果,这也是目前学者们普遍接受的观点。另一方面,对于流体的来源也存在不同的认识:BAU M<sup>[34]</sup> 和 IRBER W<sup>[72]</sup> 认为岩浆演化晚期出溶的富 F 流体与熔体发生了相互作用,稀土的氟络合物对四分组效应的形成具有重要作用。由于在与花岗岩相关的萤石脉中未发现与上凸式四分组效应互补的下凹式四分组配分模式,因而 MONECKE 等<sup>[114]</sup> 认为高硅花岗岩的四分组效应继承了与熔体相互作用的外部流体的特征。CHEN B 等<sup>[38]</sup> 对江西大湖塘钨矿田石门寺岩体和曾家垅岩体开展了 Li-Nd 同位素研究,发现具有四分组效应的曾家垅岩体(图 5)明显富集<sup>7</sup>Li,由于高  $\delta^7\text{Li}$  值与岩浆流体出溶模式不相符,且发现曾家垅岩体早期结晶磷灰石也显示四分组效应,因此认为引起四分组效应的流体可能来源于外部流体。

除异常的稀土元素配分模式外,高硅花岗岩的 Nb/Ta、Zr/Hf、K/Rb、Y/Ho 值也明显偏离普通花岗岩的范围。Nb、Ta 在元素周期表中均是第五副族元素,同属高场强元素,具有相同的电价(+5)、相似的离子半径(均为 0.64 Å)和相近的负电性(分别为 1.6 和 1.5),因而地球化学行为相似。Nb/Ta 值在岩浆演化过程中基本保持不变,各地质储库 Nb/Ta 值分布在一定范围内(图 6),其中大陆地壳的平均 Nb 含量为  $8 \times 10^{-6}$ ,Ta 含量为  $0.7 \times 10^{-6}$ ,Nb/Ta 值为 12~13<sup>[115]</sup>。

普通花岗岩整体具有比大陆地壳略低的 Nb/Ta 值,平均值为 10 左右<sup>[39]</sup>。高硅花岗岩具有明显低的 Nb/Ta 值(<10),如大兴安岭卧都河岩体 Nb/Ta 值为 5.1~10.2<sup>[36]</sup>,华南雅山岩体 Nb/Ta 值为 0.37~4.91<sup>[26]</sup>,千里山岩体晚期高硅花岗岩 Nb/Ta 值为 1.06~4.89,明显低于主体粗粒似斑状黑云母花岗岩(约 10)<sup>[30]</sup>。与稀有金属成矿相关的花岗岩

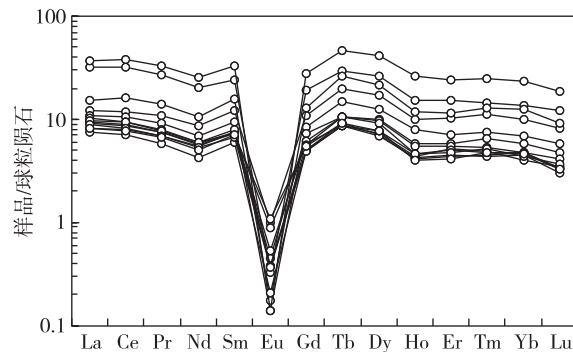


图 5 赣北曾家垅岩体显示出明显的稀土元素四分组效应(数据引自文献<sup>[38]</sup>,球粒陨石标准化值引自文献<sup>[109]</sup>)

Fig. 5 The Zengjialong pluton in northern Jiangxi Province showing REE tetrad effect (data from reference<sup>[38]</sup>, chondrite normalization values are from reference<sup>[109]</sup>)

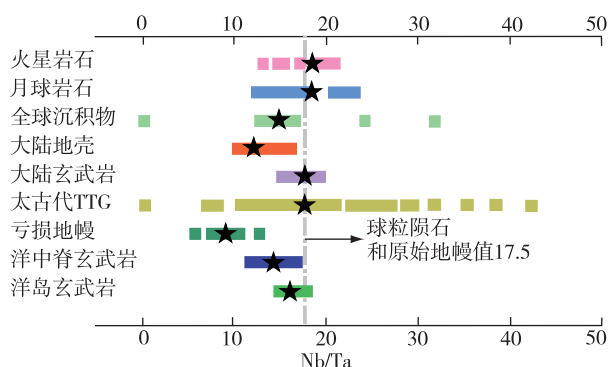


图 6 太阳系中不同岩石类型的 Nb/Ta 比值<sup>[116]</sup>

Fig. 6 Nb/Ta ratios of different rock types in the solar system<sup>[116]</sup>

具有更低的 Nb/Ta 值(<5, 图 7)<sup>[39]</sup>。对于稀有金属花岗岩低 Nb/Ta 值的原因,目前仍存在较大争议。一种观点认为岩浆分异是形成高 Ta、低 Nb/Ta 值的原因<sup>[117-118]</sup>。花岗岩中 Nb、Ta 的赋存矿物除主要矿物(云母)外,还有金红石、钛铁矿以及铌钽铁矿等副矿物。云母(富 Ti)的分离结晶使得残余熔体中 Ti 含量快速下降,抑制了含钛氧化物(金红石、钛铁矿)的饱和结晶<sup>[67]</sup>。另外,相对于 Nb,金红石和钛铁矿均更加富集 Ta<sup>[119]</sup> ( $D_{\text{Nb}}/D_{\text{Ta}} < 1$ )。因此,金红石和钛铁矿的分离结晶将导致残余熔体 Nb/Ta 值升高。花岗岩 Nb/Ta 值随演化程度增加而降低,表明金红石和钛铁矿并非控制其 Nb/Ta 值变化的主要因素<sup>[67]</sup>。一些学者认为铌铁矿和钽铁

矿溶解度的差异(铌铁矿比钽铁矿溶解度低)可能是 Nb/Ta 值变化的原因<sup>[120-122]</sup>。然而,实验研究表明,铌铁矿和钽铁矿在熔体中均具有很高的溶解度<sup>[120,123]</sup>,暗示它们在高演化熔体中很难在早期发生饱和沉淀,因此也不太可能是 Nb/Ta 值变化的主要原因。

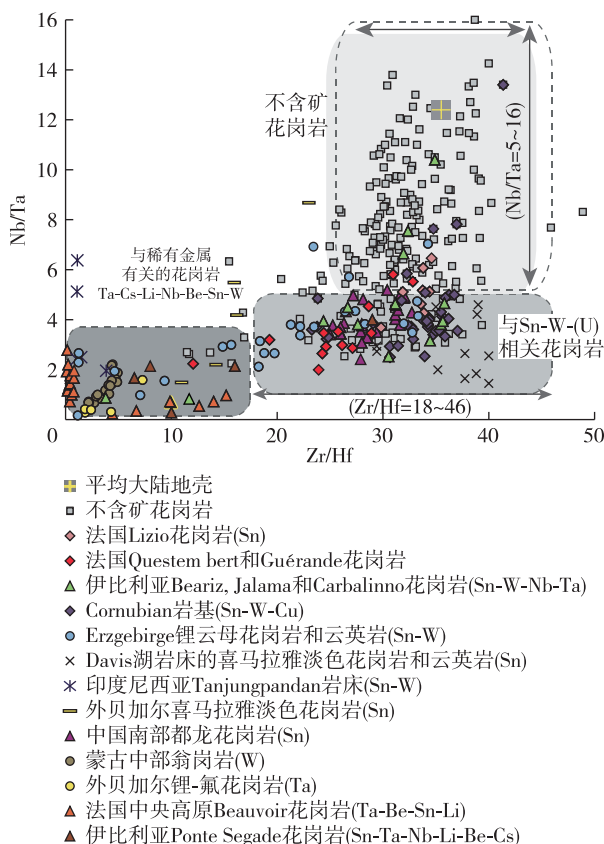


图 7 花岗岩 Zr/Hf 和 Nb/Ta 值关系图<sup>[39]</sup>

Fig. 7 Plot of Zr/Hf and Nb/Ta ratios for barren and ore-bearing peraluminous granites<sup>[39]</sup>

云母是花岗岩中常见的主要矿物,由于云母更富集 Nb( $D_{Nb}/D_{Ta} > 1$ ),因此 STEPANOV A 等<sup>[67]</sup>提出黑云母和白云母的分离结晶是稀有金属花岗岩具有低 Nb/Ta 值的关键原因。GAO M D 等<sup>[124]</sup>最新实验研究表明,云母的  $D_{Nb}$ 、 $D_{Ta}$  以及  $D_{Nb}/D_{Ta}$  (1.01~2.15)与熔体成分有关,均随着熔体聚合度的增加而升高,即高硅熔体中黑云母的分离可以更有效地降低残余熔体中的 Nb/Ta 值,且在此基础上通过模拟指出经过 99% 的分离结晶,熔体的 Nb/Ta 值可从 10~13 降至 1 左右。需要注意的是,尽管云母的分离结晶可以有效降低熔体的 Nb/Ta 值,但需要极高的分离结晶程度(>90%)。数值模拟表明,

当岩浆房中晶体含量(体积分数)超过 70%~75% 时,由于达到颗粒锁定阈值而不能发生有效晶体-熔体分离<sup>[69,125]</sup>。因此,BALLOUARD C 等<sup>[39]</sup>指出极低的 Nb/Ta 值需要母岩浆经历>90% 的分离结晶,由于如此高程度的分离结晶在现实中难以发生,进而提出岩浆-热液过程是控制高硅花岗岩具有极低 Nb/Ta 值的机制。一些实验研究显示 Nb、Ta 的流体活动较弱,不能对 Nb、Ta 富集和分异产生影响<sup>[126]</sup>。然而,ZARAISKY G P 等<sup>[127]</sup>的实验表明,Nb、Ta 在还原、富 F 流体中的溶解度比在氧化、低 F 流体中要高 3 个数量级,且相对于 Ta, Nb 具有更高的溶解度。因此,富 F 流体可以有效搬运 Nb、Ta,并产生显著的 Nb/Ta 分异。DOSTAL J 等<sup>[128]</sup>对 Davis Lake 岩体的研究也显示,Nb/Ta 值(尤其是 Nb/Ta<6 时)随 F 含量的升高而降低,表明 F 与 Nb/Ta 分异密切相关。富 F 是高硅花岗岩的重要特征之一,其出溶流体也同样为富 F 流体<sup>[30-31,129]</sup>。

### 3.3 矿物结构及成分特征

锆石是花岗岩中常见的副矿物,由于性质稳定且具有较高的封闭温度,其富含 U 和 Th 以及低普通 Pb,是开展 U-Pb 定年最常见和最有效的矿物之一。岩浆锆石一般具有典型的震荡环带,其宽度可能与锆石结晶时的温度有关<sup>[130]</sup>。然而,高硅花岗岩中的锆石无明显震荡环带,呈斑杂状、泡沫状结构,且锆石整体在 CL 图像下发黑。这些锆石在拉曼光谱下不同程度地缺失锆石特征峰<sup>[20]</sup>,表明其发生了不同程度的蜕晶作用。这是由于高硅花岗岩中的锆石富集 U、Th,大量放射性损伤导致锆石发生蜕晶化作用,从而造成其物理性质的改变,如溶解性和不透明度增加等<sup>[131-132]</sup>。由于高 U 锆石的基体效应会使 Pb 更容易被激发,从而造成 Pb/U 值的不同<sup>[133-134]</sup>。另一方面,放射性损伤和后期的蚀变引起了铅丢失,从而破坏了锆石原有的 U-Pb 体系<sup>[135]</sup>。因此,高硅花岗岩中的锆石经常无法获得有效的谐和年龄。

高硅花岗中的锆石除具有异常的结构特征外,其稀土元素含量也显著不同于一般岩浆岩中的锆石。稀土元素离子半径从  $\text{La}^{3+}$  到  $\text{Lu}^{3+}$  逐渐减小, $\text{Zr}^{4+}$  的离子半径与重稀土元素接近<sup>[136]</sup>,因此理论上锆石亏损轻稀土元素而富集重稀土元素。由于 Ce 和 Eu 为变价元素,岩浆锆石常显示正的 Ce 异常,Eu 表现为负异常或无异常。但不同于一般岩浆

岩中的锆石,高硅花岗岩中的锆石更富集轻稀土元素,具有高的La含量和 $(La/Sm)_N$ 值<sup>[137-138]</sup>。REED R等<sup>[139]</sup>对过铝质二长花岗质熔体与共存的富Cl流体开展了实验研究(800 °C, 200 MPa),结果显示轻稀土元素更易进入富Cl流体中。从富集稀土元素的热液流体中结晶出的锆石,或受热液流体交代的锆石均具有富集轻稀土的特征<sup>[140]</sup>。另外,高硅花岗岩中锆石的Th/U值(<1)<sup>[137,141]</sup>显著低于岩浆锆石的Th/U值(约为1)<sup>[130]</sup>,这是由于U在流体中的活动性比Th强,所以流体一般富U而贫Th<sup>[142-143]</sup>。

流体出溶过程除了被锆石记录外,其他造岩矿物中同样也有记录。笪昊翔等<sup>[144]</sup>对皖南伏岭高硅花岗岩体中的钾长石研究表明,从低演化花岗岩至高演化花岗岩,钾长石的K/Rb值、K/Cs值降低,而Rb、Cs含量升高。尽管分离结晶可以解释观察到的K/Rb、K/Cs和Rb、Cs含量的变化,但这需要初始熔体发生>95%的分离结晶,如此高程度的分离结晶作用似乎难以发生<sup>[4]</sup>。更重要的是,由于Pb主要赋存于钾长石中,花岗岩发生大量钾长石分离结晶时,残余熔体的Pb含量将显著降低<sup>[75]</sup>。然而,在伏岭岩体演化程度最高的花岗岩中,钾长石的Pb含量反而升高(图8)。考虑到Pb具有极强的流体活动性( $D_{Pb}^{\text{流体/熔体}} = 5.6 \sim 76$ )<sup>[145]</sup>,因此笪昊翔等<sup>[144]</sup>指出高Pb钾长石的形成需要富Pb出溶流体的参与。

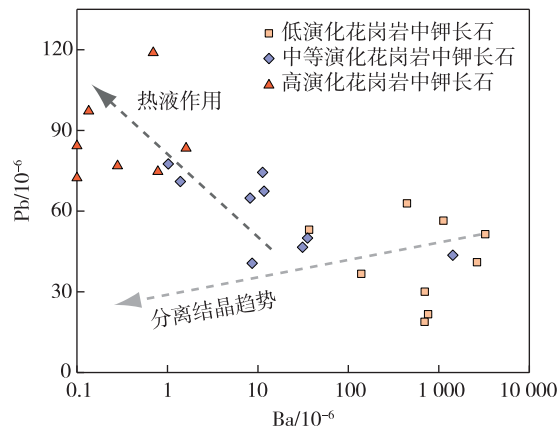


图8 皖南伏岭岩体钾长石Ba-Pb图解<sup>[144]</sup>

Fig. 8 Ba-Pb diagram of K-feldspar in Fuling pluton, southern Anhui Province<sup>[144]</sup>

### 3.4 金属稳定同位素

近年来,随着多接收电感耦合等离子体质谱

(MC-ICPMS)分析技术的快速发展,金属稳定同位素的测定也取得了重大进展,并已广泛应用于高温岩浆过程—近地表低温过程研究中<sup>[146-150]</sup>。已有研究表明,金属稳定同位素在高温岩浆过程中不发生明显分馏<sup>[151-153]</sup>。然而,花岗岩由于形成温度低(<850 °C),且经历分离结晶、流体出溶、缓慢冷却等过程,可发生明显的同位素分馏<sup>[154]</sup>,尤其是高硅花岗岩体系,由于富集H<sub>2</sub>O、F、Cl、B等挥发分,因而具有较低的结晶温度(低至600°C左右)<sup>[8]</sup>。因此,高硅花岗岩常表现出偏离一般岩浆岩的金属稳定同位素(如Li、Ba、Fe等稳定同位素<sup>[38,75,155]</sup>)特征。不同于放射性同位素,岩浆演化过程(如分离结晶、流体出溶、岩浆去气等)均可能产生金属稳定同位素的分馏,使其在示踪岩浆演化过程方面具有较大的优势和潜力。

#### 3.4.1 Li同位素

Li是最轻的碱金属元素,具有与镁离子相近的离子半径,在矿物中能够与镁发生类质同像替代<sup>[156]</sup>。Li属于中等不相容元素,在部分熔融和分离结晶过程中会优先富集在熔体中。因此,Li在地幔中的含量较低(平均值约为 $1.5 \times 10^{-6}$ )<sup>[157-158]</sup>,而在地壳中含量较高,其中Li在洋壳中的平均含量约为 $10 \times 10^{-6}$ ,Li在大陆地壳中的平均含量约为 $18 \times 10^{-6}$ <sup>[159]</sup>。另外,Li是流体活动性元素,在卤水、海底热液、岩浆热液和变质流体中均具有较高含量<sup>[160-161]</sup>。

Li有<sup>6</sup>Li和<sup>7</sup>Li两个稳定同位素,其相对丰度分别为7.52%和92.48%。Li同位素数据一般表示为样品相对标准参考物质同位素比值的千分差,现在多用 $\delta^{7}\text{Li}$ 表示,即 $\delta^{7}\text{Li} = [({}^7\text{Li}/{}^6\text{Li})_{\text{样品}} / ({}^7\text{Li}/{}^6\text{Li})_{\text{标准参考物质}} - 1] \times 1000 (\%)$ 。<sup>6</sup>Li和<sup>7</sup>Li之间相对质量差异高达16%,导致地质过程可以产生显著的Li同位素分馏,不同地质储库的Li同位素分馏可达80‰<sup>[162]</sup>。地球原始地幔的 $\delta^{7}\text{Li}$ 平均值约为+3.5‰<sup>[153]</sup>,上地幔的 $\delta^{7}\text{Li}$ 平均值约为+4‰<sup>[163-164]</sup>,洋壳的 $\delta^{7}\text{Li}$ 平均值约为+4‰<sup>[151]</sup>。相对于地幔和洋壳,大陆地壳具有相对较轻的Li同位素组成, $\delta^{7}\text{Li}$ 值为0~+4‰<sup>[159,165]</sup>。

TENG F Z等<sup>[154,166]</sup>分析并统计了A型、I型和S型花岗岩的Li同位素组成,结果显示不同类型花岗岩具有相似的 $\delta^{7}\text{Li}$ 值(平均值约为2.0‰)。由于花岗岩的 $\delta^{7}\text{Li}$ 与分异程度无关(如SiO<sub>2</sub>、Li、Rb等地球化学指标),该研究指出花岗岩的Li同位素组成变化反映了源区成分的变化。然而,越来越多的

研究表明,高硅花岗岩的 Li 同位素变化也与岩浆演化程度有关。如,赣北的  $\delta^7\text{Li}$  值地区演化程度更高的曾家垅二云母花岗岩的  $\delta^7\text{Li}$  值 ( $-0.18\text{\textperthousand} \sim +1.53\text{\textperthousand}$ ) 明显高于大湖塘矿田石门寺二云母花岗岩的  $\delta^7\text{Li}$  值 ( $-3.86\text{\textperthousand} \sim -2.71\text{\textperthousand}$ )<sup>[38]</sup>;西华山和雅山复式岩体中高演化的白云母/锂云母花岗岩的  $\delta^7\text{Li}$  值 ( $+1.9\text{\textperthousand} \sim +4.4\text{\textperthousand}$ ) 比黑云母花岗岩的  $\delta^7\text{Li}$  值 ( $-0.2\text{\textperthousand} \sim +0.7\text{\textperthousand}$ ) 具有更高的 Li 同位素组成<sup>[73]</sup>,且西华山岩体演化程度较高的花岗岩更加富集重 Li 同位素<sup>[167]</sup>;华北克拉通南缘荆山淡色花岗岩具有较高的  $\delta^7\text{Li}$  值 ( $+4.0\text{\textperthousand} \sim +9.0\text{\textperthousand}$ )<sup>[168]</sup>(图 9)。以上研究表明,经历高度分异的花岗岩整体上比低演化花岗岩更加富集重 Li 同位素。需要指出的是,由于花岗岩 Li 同位素变化范围较大,该特征仅在同一岩体或同一演化体系岩体中表现显著(图 9)。

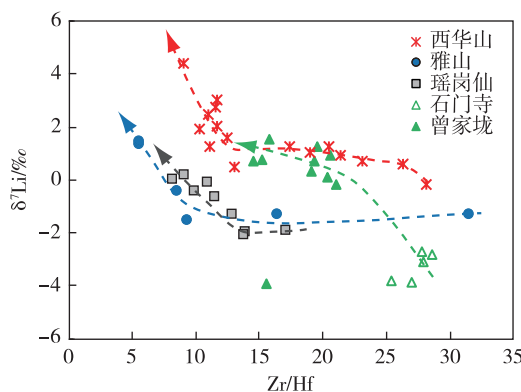


图 9 华南燕山期复式岩体 Li 同位素随 Zr/Hf 变化图解<sup>[38,73,167]</sup>

Fig. 9 Diagram of Li isotope variation with Zr/Hf in Yanshanian complex massif in South China<sup>[38,73,167]</sup>

多数学者认为,分离结晶作用对花岗岩 Li 同位素分馏影响不大<sup>[38,73,154]</sup>。由于高硅花岗岩常伴随流体出溶作用,因此流体-熔体或流体-岩石作用是研究 Li 同位素分馏机制关注的重点。Li 是强流体质元素,其流体/熔体分配系数可达  $1.8 \sim 40.6$ <sup>[145]</sup>。Li 在流体和熔体中的络合形式不同,会产生明显的同位素分馏。但是,关于流体出溶过程中 Li 同位素的分馏行为却有不同的认识:VLASTÉLIC 等<sup>[169]</sup>对一套经历去气作用的火山岩开展了 Li 同位素研究,发现未去气玄武岩的  $\delta^7\text{Li}$  值约为  $+4.5\text{\textperthousand}$ ,而去气的浮岩 Li 同位素低至约  $-20\text{\textperthousand}$ ,据此认为从岩浆中逃逸的富水气体富集

${}^7\text{Li}(\alpha^{\text{V}-\text{M}}$  被估计为 1.010)。XIANG L 等<sup>[85]</sup>对华南元宝山高硅花岗岩的研究发现,分布于晶洞中的电气石具有更高的  $\delta^7\text{Li}$  值,认为出溶流体更加富集 ${}^7\text{Li}$ 。但也有一些学者指出花岗质熔体出溶流体可能更加富集 ${}^6\text{Li}$ :FAN J J 等<sup>[170]</sup>发现新疆白龙山富锂伟晶岩和贫锂伟晶岩之间的 Li 同位素分馏显著,认为这是花岗质岩浆演化晚期的流体出溶造成的,熔体由于 Li-Al 呈四面体配位而富集 ${}^7\text{Li}$ (形成富锂伟晶岩),Li 在流体中以较弱的水合键结合而富集 ${}^6\text{Li}$ (形成贫锂伟晶岩)。ZHANG H J 等<sup>[171]</sup>对四川甲基卡伟晶岩的研究也提出相似的观点。此外,云英岩相对花岗岩具有更低的  $\delta^7\text{Li}$ ,这也被认为是出溶流体富集 ${}^6\text{Li}$  所致<sup>[167]</sup>。最近,ELLIS B S 等<sup>[172]</sup>对美国 Bishop、希腊 Kos 地区的流纹岩和花岗岩及其中的黑云母开展了系统的 Li 同位素研究,发现黑云母具有富 Li(可达  $2300 \times 10^{-6}$  以上)、低  $\delta^7\text{Li}$ (最低可达  $-27.6\text{\textperthousand}$ ) 特征,认为低  $\delta^7\text{Li}$  的黑云母可能是在层间捕获了出溶的富 Li(且相对富 ${}^6\text{Li}$ ) 流体形成。另一方面,也有学者提出不同的分馏机制可导致 Li 同位素在流体出溶/去气过程中表现出不同的分馏行为:在平衡分馏条件下, ${}^7\text{Li}$  优先进入挥发相中;如果流体出溶/去气过程非常迅速,由于 ${}^6\text{Li}$  扩散速率比 ${}^7\text{Li}$  快约 3%,受动力分馏控制挥发相将更加富集 ${}^6\text{Li}$ <sup>[173-174]</sup>。LI X F 等<sup>[175]</sup>对南岭新田岭岩体的研究同样表明,花岗质岩浆演化后期可能发生快速流体出溶,不平衡过程导致的扩散动力分馏是晚期高硅花岗岩富集重 Li 同位素的主要机制。此外,也有学者提出外来流体与熔体之间相互作用<sup>[38]</sup>,或不平衡条件下流体-花岗岩相互作用<sup>[72]</sup>,同样可导致高硅花岗岩具有更高的 Li 同位素组成。

### 3.4.2 Ba 同位素

Ba 是一种化学性质活泼的碱土金属元素,在地幔中含量较低 ( $6.9 \times 10^{-6}$ )<sup>[176]</sup>,富集于地壳岩石中。其中,大陆地壳平均 Ba 含量为  $456 \times 10^{-6}$ ,大陆上地壳平均 Ba 含量为  $628 \times 10^{-6}$ <sup>[177]</sup>。Ba 在岩浆岩中主要赋存于钾长石和黑云母中,因此 Ba 在基性-中性岩浆中表现为不相容,而在花岗质岩浆中主要表现为相容,且 Ba 含量随演化程度的增加而降低<sup>[35,178]</sup>。同时,Ba 是流体质元素<sup>[179]</sup>,在俯冲过程中 Ba 随俯冲板片脱水释放的流体而大量进入地幔楔中<sup>[180]</sup>。

Ba 有 7 种稳定同位素: ${}^{130}\text{Ba}$ 、 ${}^{132}\text{Ba}$ 、 ${}^{134}\text{Ba}$ 、 ${}^{135}\text{Ba}$ 、 ${}^{136}\text{Ba}$ 、 ${}^{137}\text{Ba}$ 、 ${}^{138}\text{Ba}$ , 相对丰度分别为 0.106%、

0.101%、2.417%、6.592%、7.853%、11.232%、71.699%<sup>[181]</sup>。Ba同位素数据一般表示样品相对标准参考物质同位素比值的千分差,现在多用 $\delta^{138/134}\text{Ba}$ 表示, $\delta^{138/134}\text{Ba} = [(\text{样品}^{138}\text{Ba}/\text{样品}^{134}\text{Ba})/\text{标准}^{138}\text{Ba} - 1] \times 1000 (\%)$ 。NIELSEN S G 等<sup>[182]</sup>通过21件大洋玄武岩样品估计了亏损上地幔的 $\delta^{138/134}\text{Ba}$ 为(0.14±0.02)%;NAN X Y 等<sup>[183]</sup>分析了30件代表性大洋玄武岩样品,重新估算出亏损上地幔的 $\delta^{138/134}\text{Ba}$ 为(0.05±0.05)%。此外,大陆上地壳具有略低于亏损上地幔的Ba同位素组成(0.00±0.04)%<sup>[184]</sup>。花岗岩作为大陆地壳的重要组成部分,

其Ba同位素值整体位于大陆上地壳的平均范围内。例如,佛冈I型花岗岩的 $\delta^{138/134}\text{Ba}$ 为-0.21‰~0.02‰,大容山S型花岗岩 $\delta^{138/134}\text{Ba}$ 为0.04‰~0.15‰<sup>[184]</sup>,南岭骑田岭低演化第一阶段花岗岩 $\delta^{138/134}\text{Ba}$ 为-0.24‰~0.37‰<sup>[75]</sup>。相较于低演化花岗岩,高硅花岗岩的Ba同位素明显偏离大陆上地壳的平均值,整体上更加富集轻Ba同位素,例如,喜马拉雅康巴淡色花岗岩的 $\delta^{138/134}\text{Ba}$ 为-1.32‰~0.12‰<sup>[185]</sup>,南岭南昆山岩体 $\delta^{138/134}\text{Ba}$ 为-0.63‰~-0.44‰<sup>[184]</sup>,南岭骑田岭第二阶段和第三阶段高硅花岗岩 $\delta^{138/134}\text{Ba}$ 为-1.79‰~0.14‰<sup>[75]</sup>(图10)。

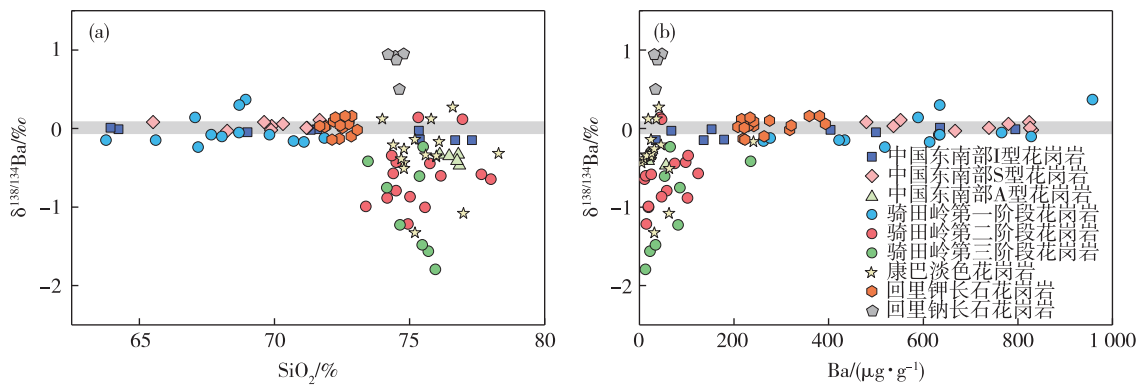


图10 花岗岩 $\delta^{138/134}\text{Ba}$ 与 $\text{SiO}_2$ (a)和Ba(b)含量关系图<sup>[73,184-186]</sup>

Fig. 10 Diagram of  $\delta^{138/134}\text{Ba}$  and  $\text{SiO}_2$ (a) and Ba(b) content of granite<sup>[73,184-186]</sup>

如前所述,高硅花岗岩经历了强烈的分离结晶作用和晚期的流体出溶作用,二者均可能导致了Ba同位素发生分馏。DENG G X 等<sup>[186]</sup>报道了胶北回里钠长花岗岩具有富集重Ba同位素的特征,其 $\delta^{138/134}\text{Ba}$ 为0.50‰~0.95‰。作为主要的含Ba矿物,钾长石具有富集轻Ba同位素的特征,因此大量钾长石的分离结晶将导致残余熔体(钠长花岗岩)富集重Ba同位素。然而,分离结晶模式并不适用于喜马拉雅康巴淡色花岗岩和南岭骑田岭岩体,鉴于角闪石、斜长石具有低的Ba含量,它们的分离结晶不会显著改变残余熔体的Ba同位素组成,而钾长石(富集轻Ba)的分离结晶则会导致残余熔体富集重Ba,但这与上述两个高硅岩体均富集轻Ba同位素相矛盾<sup>[75,185]</sup>。前人研究表明,流体作用可导致硅酸盐和流体之间Ba同位素发生明显分馏<sup>[184,187]</sup>。GUO H 等<sup>[188]</sup>进一步开展了流体出溶过程中流体-熔体Ba同位素分馏实验,结果显示 $\Delta^{138/134}\text{Ba}_{\text{流体}-\text{熔体}}$ 为-0.62‰~-0.14‰,表明相对于硅酸盐熔体,

出溶流体明显富集轻Ba同位素。WANG W Z 等<sup>[189]</sup>通过第一性原理计算了矿物-流体相互作用过程中Ba同位素的分馏行为,同样表明流体明显富集轻Ba同位素。这两项研究为高硅花岗岩富集轻Ba同位素提供了重要的理论依据。据此,HUANG F 等<sup>[185]</sup>和DENG G X 等<sup>[75]</sup>认为高硅花岗岩低 $\delta^{138/134}\text{Ba}$ 特征是流体-熔体相互作用的结果,并指出该流体-熔体相互作用并非流体出溶(离开熔体)导致,而是来源于深部晶粥体出溶流体的加入;深部低 $\delta^{138/134}\text{Ba}$ 的出溶岩浆流体改造浅部高硅熔体,使其具有流体的Ba同位素组成特征。

### 3.4.3 Fe同位素

Fe是地球的主要构成元素之一,也是岩浆岩的主要构成元素之一,主要赋存于橄榄石、辉石、角闪石、黑云母等镁铁质硅酸盐矿物以及铁钛氧化物中。由于含铁矿物的结晶分异,岩浆中的Fe含量随演化程度的增加而降低<sup>[178]</sup>。Fe在流体中的含量变化较大,这与其价态和赋存形式有关:整体上

$\text{Fe}^{2+}$ 的水溶性较大,还原性流体中含量可达 $1000 \times 10^{-6}$ 以上,而 $\text{Fe}^{3+}$ 在流体中含量极低,但在有合适络合物存在时也可有较高含量<sup>[155,190]</sup>。

Fe在自然界有4个稳定同位素: $^{54}\text{Fe}$ 、 $^{56}\text{Fe}$ 、 $^{57}\text{Fe}$ 、 $^{58}\text{Fe}$ ,其相对丰度分别为5.85%、91.76%、2.12%、0.28%。Fe同位素多用 $\delta^{56}\text{Fe}$ 报道,即 $\delta^{56}\text{Fe} = [({}^{56}\text{Fe}/{}^{54}\text{Fe})_{\text{样品}} / ({}^{56}\text{Fe}/{}^{54}\text{Fe})_{\text{标准参考物质}} - 1] \times 1000 (\%)$ 。前人分别估算了不同地质储库的Fe同位素组成,地球的铁同位素平均值为 $(-0.016 \pm 0.045)\%$ <sup>[191]</sup>,上地幔的 $\delta^{56}\text{Fe}$ 平均值为 $(0.02 \pm 0.03)\%$ <sup>[192]</sup>,洋中脊玄武岩的 $\delta^{56}\text{Fe}$ 平均值为 $(0.105 \pm 0.006)\%$ <sup>[193]</sup>,洋岛玄武岩的 $\delta^{56}\text{Fe}$ 平均值为 $(0.121 \pm 0.009)\%$ <sup>[193]</sup>。不同类型岩浆岩的 $\delta^{56}\text{Fe}$ 值为 $-0.03\% \sim 0.40\%$ ,且表现出Fe同位素随岩浆演化逐渐变重的趋势<sup>[147]</sup>。值得注意的是,从基性岩到演化程度较低的花岗岩( $\text{SiO}_2 < 74\%$ ),Fe同位素并无明显分馏,基性岩和中性岩具有相似的 $\delta^{56}\text{Fe}$ 值(平均值分别为 $(0.10 \pm 0.09)\%$ 和 $(0.09 \pm 0.11)\%$ <sup>[147,155]</sup>),而高硅花岗岩则具有明显偏重的Fe同位素组成( $\delta^{56}\text{Fe} = 0.07\% \sim 0.55\%$ ,图11)<sup>[147,155,194]</sup>。目前,对于高硅花岗岩高 $\delta^{56}\text{Fe}$ 的成因和分馏机理仍存在较大争论。有学者提出花岗岩中富集轻Fe同位素的矿物(如钛铁矿、黑云母)的分离结晶是高硅花岗岩具有高 $\delta^{56}\text{Fe}$ 的原因<sup>[194-197]</sup>。然而,富Fe矿物的分离结晶理论上主要发生在中基性岩浆阶段,但中基性岩浆以及低演化酸性岩浆中并未表现出明显的Fe同位素分馏,并且岩浆演化晚期结晶的磁铁矿一般和熔体不发生同位素分馏或具有更重的Fe同位素组成,因此分离结晶模型也面临一些解释上的问题<sup>[155,198-199]</sup>。另一方面,Fe在岩浆出溶流体过程中表现出较强的流体活动性,流体-熔体分配系数可达 $0.85 \sim 3.5$ <sup>[145]</sup>。在自然界花岗岩样品中也发现流体包裹中Fe的含量可达5.5%<sup>[200]</sup>。因此,一些学者提出高硅花岗岩的高 $\delta^{56}\text{Fe}$ 特征是由大量富 $\text{Fe}^{2+}$ (以 $\text{FeCl}_2^0$ 的形式)流体的出溶所导致<sup>[199,201-202]</sup>。由于出溶流体中主要为 $\text{Fe}^{2+}$ ,而 $\text{Fe}^{3+}$ 含量很低,因此富 $\text{Fe}^{2+}$ 流体相对更加富集轻Fe同位素<sup>[203]</sup>。前人对Fe-Cu矿床的研究发现,矽卡岩和磁铁矿均具有较低的 $\delta^{56}\text{Fe}$ 值,同样表明出溶流体富集轻Fe同位素<sup>[147,204]</sup>。流体出溶模式的另一个证据来自对伟晶岩的研究:伟晶岩(高硅花岗质岩石)通常被认为发生过极高程度

的分异演化以及流体-熔体作用<sup>[205-207]</sup>。TELUS M等<sup>[201]</sup>对Black Hills地区的伟晶岩开展了Fe-Zn同位素研究,与高硅花岗岩类似,伟晶岩样品具有较高的 $\delta^{56}\text{Fe}$ 值,且同时具有较高的 $\delta^{66}\text{Zn}$ 值。据此,他们指出流体出溶是Black Hills伟晶岩富集重Fe同位素的重要机制。

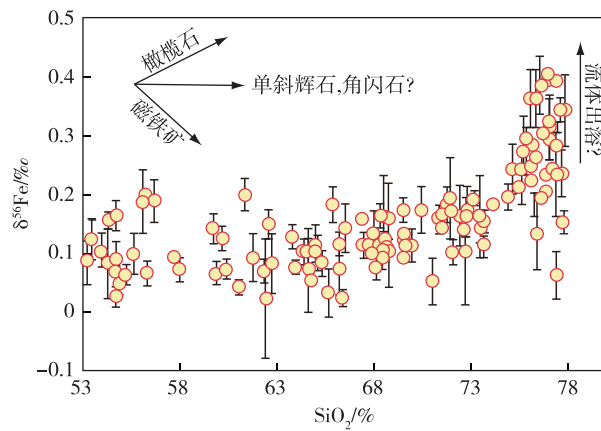


图11 中酸性岩石Fe同位素变化图<sup>[155]</sup>  
Fig. 11 Diagram of Fe isotope variation in felsic rocks<sup>[155]</sup>

如上所述,高硅花岗岩富集重Fe同位素的机制还存在很大争论。但不可否认的是,流体出溶是导致高硅花岗岩以及伟晶岩富集重Fe同位素的重要过程,因此Fe同位素是示踪高硅花岗岩流体出溶作用的重要工具。但在具体研究过程中,需要排除分离结晶作用的影响,并且与其他流体出溶指标(岩相学、地球化学等)同时使用。

#### 4 流体出溶在稀有金属成矿作用中的意义

高硅花岗岩晚期经历的流体出溶作用,将会改变其地球化学和同位素特征。同时,流体出溶对稀有金属成矿具重要意义。首先,稀有金属元素(Li、Be、W、Sn、Nb、Ta、Rb、Cs)在花岗质熔体中均为强不相容元素,因此随着岩浆的演化,这些元素在残余熔体中逐渐富集。例如,极高演化的湘南香花岭花岗岩中Li含量可超过 $2000 \times 10^{-6}$ ,Rb含量可超过 $1900 \times 10^{-6}$ ,W、Sn含量可分别达 $1000 \times 10^{-6}$ 和 $50 \times 10^{-6}$ 以上<sup>[208]</sup>。又如,BALLOUARD C等<sup>[39]</sup>的统计数据显示,高硅花岗岩中Nb、Ta含量可达 $100 \times 10^{-6}$ 以上。相比而言,稀有金属元素在地壳中的丰度要低的多( $\text{Li}=16 \times 10^{-6}$ , $\text{Rb}=49 \times 10^{-6}$ , $\text{W}=1 \times 10^{-6}$ , $\text{Sn}=1.7 \times 10^{-6}$ , $\text{Nb}=8 \times 10^{-6}$ , $\text{Ta}=$

$0.7 \times 10^{-6}$ <sup>[174]</sup>。普通花岗岩通常不具有稀有金属成矿特征,王汝成等<sup>[32]</sup>计算了由普通花岗岩( $\text{Be} = 4 \times 10^{-6}$ )演化到绿柱石结晶所需要的Be含量( $205 \times 10^{-6}$ ),需要熔体经过99%以上的分离结晶。考虑到熔体含量低于25%时不易于熔体抽离,这一演化过程需要经历至少4次75%程度的分离结晶。其次,这些稀有金属元素均为流体活动性元素,它们在流体出溶过程中均倾向于分配到流体相中。例如,最新的实验研究显示, $D_{\text{W}}$ 流体/熔体可达 $8 \sim 37$ <sup>[209-210]</sup>, $D_{\text{Sn}}$ 流体/熔体可达 $2 \sim 35$ <sup>[71]</sup>, $D_{\text{Li}}$ 流体/熔体可达 $2 \sim 40$ <sup>[145,211]</sup>, $D_{\text{Cs}}$ 流体/熔体为 $1.4 \sim 6.2$ <sup>[145]</sup>。尽管一般认为Nb、Ta在流体中的活动性较弱<sup>[212]</sup>,自然样品测得的流体/熔体分配系数也较低( $< 0.1$ )<sup>[145]</sup>,但实验研究也表明,Nb、Ta在富F热液中的溶解度和迁移能力大大提升<sup>[127]</sup>。因此,对于富F的高硅花岗岩体系,Nb、Ta在流体中是易于迁移的。在经过熔体富集和流体出溶两个过程之后,出溶的热液流体将富集稀有金属元素,在岩体周围形成相关的稀有金属矿床。

## 5 主要认识及展望

(1)高硅花岗岩普遍经历高程度分异演化,不可避免发生流体饱和出溶。

(2)晶洞构造、雪球结构和单向固结结构是高硅花岗岩经历流体出溶较为明确的证据。但这些结构构造仅在高硅花岗岩体局部发育,流体出溶的识别更多地需要依赖全岩和矿物地球化学证据。

(3)全岩稀土四分组效应以及极低的Nb/Ta、Zr/Hf和K/Rb值,是识别流体出溶作用的有效指标。

(4)矿物学方面,锆石发生蜕晶化作用,富集轻稀土元素,甚至发育稀土元素的四分组效应,均指示了热液流体的参与。高演化钾长石的富Pb特征指示形成于热液流体参与的环境。但流体出溶的矿物学记录不限于本文列举的锆石和钾长石,其他矿物(如云母、电气石、铌钽铁矿、磷灰石等)同样可以记录该过程。相比于全岩分析,矿物的精细解剖是识别流体出溶过程更为有效的手段。

(5)Li、Ba、Fe同位素在高硅花岗岩中发生明显分馏,相对而言,高硅花岗岩富集重Li、轻Ba和重Fe同位素,这很可能是花岗质熔体演化晚期流体-熔体相互作用的结果,但有多种因素可能影响金属

稳定同位素分馏,因而其成因仍存在较大争论。流体出溶过程中同位素分馏的实验研究和模拟计算(如第一性原理计算)至关重要,是利用金属稳定同位素识别流体出溶过程的基石。

**致谢:**感谢两位评审专家和邢光福主编对本文提出的宝贵修改意见和建议。

## 参考文献

- [1] CAMPBELL I H, TAYLOR S R. No water, no granites-No oceans, no continents [J]. Geophysical Research Letters, 1983, 10(11): 1061-1064.
- [2] GLAZNER A F, COLEMAN D S, BARTLEY J M. The tenuous connection between high-silica rhyolites and granodiorite plutons[J]. Geology, 2008, 36(2): 183-186.
- [3] CHEN S C, YU J J, BI M F. Extraction of fractionated interstitial melt from a crystal mush system generating the Late Jurassic high-silica granites from the Qitianling composite pluton, South China: implications for greisen-type tin mineralization [J]. Lithos, 2021, 382: 105952.
- [4] BACHMANN O, BERGANTZ G W. On the origin of crystal-poor rhyolites: extracted from batholithic crystal mushes [J]. Journal of Petrology, 2004, 45(8): 1565-1582.
- [5] CASHMAN K V, SPARKS R S J, BLUNDY J D. Vertically extensive and unstable magmatic systems: a unified view of igneous processes[J]. Science, 2017, 355(6331): 1-11.
- [6] 马昌前,李艳青.花岗岩体的累积生长与高结晶度岩浆的分异[J].岩石学报,2017,33(5):1479-1488.  
MA C Q, LI Y Q. Incremental growth of granitoid plutons and highly crystalline magmatic differentiation[J]. Acta Petrologica Sinica, 2017, 33(5): 1479-1488.
- [7] 吴福元,刘小驰,纪伟强,等.高分异花岗岩的识别与研究[J].中国科学(地球科学),2017,47(7):745-765.  
WU F Y, LIU X C, JI W Q, et al. Highly fractionated granites: recognition and research[J]. Science China (Earth Sciences), 2017, 47(7): 745-765.
- [8] 吴福元,郭春丽,胡方泱,等.南岭高分异花岗岩成岩与成矿[J].岩石学报,2023,39(1):1-36.  
WU F Y, GUO C L, HU F Y, et al. Petrogenesis of the highly fractionated granites and their mineralizations in Nanling Range[J]. Acta Petrologica

- Sinica, 2023, 39(1): 1-36.
- [9] THOMAS R, DAVIDSON P. Water in granite and pegmatite-forming melts [J]. *Ore Geology Reviews*, 2012, 46: 32-46.
- [10] EDMONDS M, WOODS A W. Exsolved volatiles in magma reservoirs [J]. *Journal of Volcanology and Geothermal Research*, 2018, 368: 13-30.
- [11] THOMAS R, DAVIDSON P, APPEL K. The enhanced element enrichment in the supercritical states of granite-pegmatite systems [J]. *Acta Geochimica*, 2019, 38: 335-349.
- [12] 王国光, 倪培, 潘君屹. 花岗质岩石相关成矿系统的流体作用[J]. *矿物岩石地球化学通报*, 2020, 39(3): 463-471.  
WANG G G, NI P, PAN J Y. Fluid characteristics of granite-related ore forming systems [J]. *Bulletin of Mineralogy, Petrology and Geochemistry*, 2020, 39(3): 463-471.
- [13] AUDÉTAT A. The metal content of magmatic-hydrothermal fluids and its relationship to mineralization potential [J]. *Economic Geology*, 2019, 114(6): 1033-1056.
- [14] 郭素淑, 李曙光. 淡色花岗岩的岩石学和地球化学特征及其成因[J]. *地学前缘*, 2007, 14(6): 290-298.  
GUO S S, LI S G. Petrological and geochemical constraints on the origin of leucogranites [J]. *Earth Science Frontiers*, 2007, 14(6): 290-298.
- [15] 吴福元, 刘志超, 刘小驰, 等. 喜马拉雅淡色花岗岩[J]. *岩石学报*, 2015, 31(1): 1-36.  
WU F Y, LIU Z C, LIU X C, et al. Himalayan leucogranite: petrogenesis and implications to orogenesis and plateau uplift [J]. *Acta Petrologica Sinica*, 2015, 31(1): 1-36.
- [16] 刘鹏, 张德会, 吴鸣谦, 等. 浅谈花岗岩浆热液的形成及成矿作用[J]. *地质论评*, 2020, 66(3): 699-719.  
LIU P, ZHANG D H, WU M Q, et al. Discussion on magma—hydrothermal formation and mineralization of granites [J]. *Geological Review*, 2020, 66(3): 699-719.
- [17] WU F Y, LIU X C, LIU Z C, et al. Highly fractionated Himalayan leucogranites and associated rare-metal mineralization [J]. *Lithos*, 2020, 352/353: 1-24.
- [18] CAO H W, PEI Q M, SANTOSH M, et al. Himalayan leucogranites: a review of geochemical and isotopic characteristics, timing of formation, genesis, and rare metal mineralization [J]. *Earth-Science Reviews*, 2022, 234: 1-28.
- [19] CANDELA P A. A review of shallow, ore-related granites: textures, volatiles, and ore metals [J]. *Journal of Petrology*, 1997, 38(12): 1619-1633.
- [20] WANG Z Q, CHEN B, MA X H. Petrogenesis of the Late Mesozoic Guposhan composite plutons from the Nanling Range, South China: implications for W-SN mineralization [J]. *American Journal of Science*, 2014, 314(1): 235-277.
- [21] SUN K K, CHEN B, DENG J. Biotite in highly evolved granites from the Shimensi W-Cu-Mo polymetallic ore deposit, China: insights into magma source and evolution [J]. *Lithos*, 2019, 350/351: 105245.
- [22] 王汝成, 谢磊, 诸泽颖, 等. 云母: 花岗岩-伟晶岩稀有金属成矿作用的重要标志矿物[J]. *岩石学报*, 2019, 35(1): 69-75.  
WANG R C, XIE L, ZHU Z Y, et al. Micas: important indicators of granite-pegmatite-related rare-metal mineralization [J]. *Acta Petrologica Sinica*, 2019, 35(1): 69-75.
- [23] XIE L, WANG Z J, WANG R C, et al. Mineralogical constraints on the genesis of W-Nb-Ta mineralization in the Laiziling granite (Xianghualing district, South China) [J]. *Ore Geology Reviews*, 2018, 95: 695-712.
- [24] LI J, HUANG X L, FU Q, et al. Tungsten mineralization during the evolution of a magmatic-hydrothermal system: mineralogical evidence from the Xihuashan rare-metal granite in South China [J]. *American Mineralogist*, 2021, 106(3): 443-460.
- [25] YIN R, HUANG X L, WANG R C, et al. Rare-metal enrichment and Nb-Ta fractionation during magmatic-hydrothermal processes in rare-metal granites: evidence from zoned micas from the Yashan pluton, South China [J]. *Journal of Petrology*, 2022, 63(10): 1-28.
- [26] 李洁, 黄小龙. 江西雅山花岗岩岩浆演化及其 Ta-Nb 富集机制[J]. *岩石学报*, 2013, 29(12): 4311-4322.  
LI J, HUANG X L. Mechanism of Ta-Nb enrichment and magmatic evolution in the Yashan granites, Jiangxi Province, South China [J]. *Acta Petrologica Sinica*, 2013, 29(12): 4311-4322.
- [27] ZHU J C, LI R K, LI F C, et al. Topaz-albite granites and rare-metal mineralization in the Limu district, Guangxi Province, southeast China [J]. *Mineralium Deposita*, 2001, 36: 393-405.
- [28] HUANG F F, WANG R C, XIE L, et al. Differentiated rare-element mineralization in an ongonite—

- topazite composite dike at the Xianghualing tin district, Southern China: an electron-microprobe study on the evolution from niobium-tantalum-oxides to cassiterite[J]. *Ore Geology Reviews*, 2015, 65: 761-778.
- [29] LEE C T A, MORTON D M. High silica granites: terminal porosity and crystal settling in shallow magma chambers[J]. *Earth and Planetary Science Letters*, 2015, 409: 23-31.
- [30] CHEN B, MA X H, WANG Z Q. Origin of the fluorine-rich highly differentiated granites from the Qianlishan composite plutons (South China) and implications for polymetallic mineralization[J]. *Journal of Asian Earth Sciences*, 2014, 93: 301-314.
- [31] 孙建东,徐敏成,谭桂丽,等.赣东北黄山铌钽矿床成矿岩体地球化学特征及成矿意义[J].华东地质,2023,44(1):28-38.
- SUN J D, XU M C, TAN G L, et al. Geochemical characteristics and metallogenic significance of Huangshan Nb-Ta deposit in northeast Jiangxi Province[J]. *East China Geology*, 2023, 44(1): 28-38.
- [32] 王汝成,吴福元,谢磊,等.藏南喜马拉雅淡色花岗岩稀有金属成矿作用初步研究[J].中国科学(地球科学),2017, 47(8): 871-880.
- WANG R C, WU F Y, XIE L, et al. A preliminary study of rare-metal mineralization in the Himalayan leucogranite belts, South Tibet [J]. *Science China (Earth Sciences)*, 2017, 47(8): 871-880.
- [33] HALLIDAY A N, DAVIDSON J P, HILDRETH W, et al. Modelling the petrogenesis of high Rb/Sr silicic magmas [J]. *Chemical Geology*, 1991, 92 (1/3): 107-114.
- [34] BAU M. Controls on the fractionation of isovalent trace elements in magmatic and aqueous systems: evidence from Y/Ho, Zr/Hf, and lanthanide tetrad effect [J]. *Contributions to Mineralogy and Petrology*, 1996, 123(3): 323-333.
- [35] 王炯辉,马星华,李毅,等.花岗质复式岩体成因及其与W-Mo成矿的关系——以广西油麻坡岩体为例[J].地质学报,2014, 88(7): 1219-1235.
- WANG J H, MA X H, LI Y, et al. Petrogenesis of granitic complexes and implications for the W-Mo mineralization: a case study from the Youmapo Pluton, Guangxi Province[J]. *Acta Geologica Sinica*, 2014, 88 (7): 1219-1235.
- [36] JAHN B, WU F Y, CAPDEVILA R, et al. Highly evolved juvenile granites with tetrad REE patterns: the Woduhe and Baerzhe granites from the Great Xing'an Mountains in NE China [J]. *Lithos*, 2001, 59 (4): 171-198.
- [37] WU F Y, JAHN B, WILDE S A, et al. Highly fractionated I-type granites in NE China (I): geochronology and petrogenesis[J]. *Lithos*, 2003, 66 (3-4): 241-273.
- [38] CHEN B, GU H O, CHEN Y J, et al. Lithium isotope behaviour during partial melting of metapelites from the Jiangnan Orogen, South China: implications for the origin of REE tetrad effect of F-rich granite and associated rare-metal mineralization[J]. *Chemical Geology*, 2018, 483: 372-384.
- [39] BALLOUARD C, POUJOL M, BOULVAIS P, et al. Nb-Ta fractionation in peraluminous granites: a marker of the magmatic-hydrothermal transition[J]. *Geology*, 2016, 44(3): 231-234.
- [40] GUO C L, CHEN Y C, ZENG Z L, et al. Petrogenesis of the Xihuashan granites in Southeastern China: constraints from geochemistry and in-situ analyses of zircon U-Pb-Hf-O isotopes[J]. *Lithos*, 2012, 148: 209-227.
- [41] 陈伟,陈斌,孙克克.江西彭山锡多金属矿集区曾家垄锡矿相关的铅质花岗岩成因[J].地球化学,2018, 47(5): 554-574.
- CHEN W, CHEN B, SUN K K. Petrogenesis of the Zengjialong highly differentiated granite in the Pengshan Sn-polymetallic ore field, Jiangxi Province [J]. *Geochimica*, 2018, 47(5): 554-574.
- [42] WEINBERG R F. Himalayan leucogranites and migmatites: nature, timing and duration of anatexis[J]. *Journal of Metamorphic Geology*, 2016, 34 (8): 821-843.
- [43] HOPKINSON T N, HARRIS N B W, WARREN C J, et al. The identification and significance of pure sediment-derived granites[J]. *Earth and Planetary Science Letters*, 2017, 467: 57-63.
- [44] 曾令森,高利娥.喜马拉雅碰撞造山带新生代地壳深熔作用与淡色花岗岩[J].岩石学报,2017, 33 (05): 1420-1444.
- ZENG L S, GAO L E. Cenozoic crustal anatexis and the leucogranites in the Himalayan collisional orogenic belt[J]. *Acta Petrologica Sinica*, 2017, 33 (5): 1420-1444.
- [45] 朱金初,王汝成,陆建军,等.湘南癞子岭花岗岩体分异演化和成岩成矿[J].高校地质学报,2011, 17(3): 381-392.
- ZHU J C, WANG R C, LU J J, et al. Fractionation,

- evolution, petrogenesis and mineralization of Laiziling granite pluton, Southern Hunan Province [J]. Geological Journal of China Universities, 2011, 17(3): 381-392.
- [46] 周新民,陈培荣,徐夕生,等.南岭地区晚中生代花岗岩成因与岩石圈动力学演化[M].北京:科学出版社,2007.
- ZHOU X M, CHEN P R, XU X S, et al. Gensis of Late Mesozoic granites and lithospheric dynamic evolution in Nanling area [M]. Beijing: Science Press, 2007.
- [47] GUO N X, ZHAO Z, GAO J F, et al. Magmatic evolution and W-Sn-U-Nb-Ta mineralization of the Mesozoic Jiulongnao granitic complex, Nanling Range, South China [J]. Ore Geology Reviews, 2018, 94: 414-434.
- [48] 张旗.花岗质岩浆能够结晶分离和演化吗? [J].岩石矿物学杂志,2012,31(2): 252-260.
- ZHANG Q. Could granitic magmas experience fractionation and evolution? [J]. Acta Petrologica et Mineralogica, 2012, 31(2): 252-260.
- [49] 张旗,潘国强,李承东,等.花岗岩结晶分离作用问题——关于花岗岩研究的思考之二[J].岩石学报,2007,23(6): 1239-1251.
- ZHANG Q, PAN G Q, LI C D, et al. Does fractional crystallization occur in granitic magma some crucial questions on granite study (2) [J]. Acta Petrologica Sinica, 2007, 23(6): 1239-1251
- [50] PUTIRKA K D, CANCHOLA J, RASH J, et al. Pluton assembly and the genesis of granitic magmas: insights from the GIC pluton in cross section, Sierra Nevada Batholith, California[J]. American Mineralogist, 2014, 99(7): 1284-1303.
- [51] FIEDRICH A M, BACHMAMANN O, ULMER P, et al. Mineralogical, geochemical, and textural indicators of crystal accumulation in the Adamello Batholith (Northern Italy) [J]. American Mineralogist, 2017, 102(12): 2467-2483.
- [52] GELMAN S E, DEERING C D, BACHMANN O, et al. Identifying the crystal graveyards remaining after large silicic eruptions[J]. Earth and Planetary Science Letters, 2014, 403: 299-306.
- [53] BARNES C G, ERNST W G, BERRY R, et al. Petrology and geochemistry of an upper crustal pluton: a view into crustal-scale magmatism during arc to retro-arc transition[J]. Journal of Petrology, 2016, 57(7): 1361-1388.
- [54] ANNEN C. From plutons to magma chambers: thermal constraints on the accumulation of eruptible silicic magma in the upper crust[J]. Earth and Planetary Science Letters, 2009, 284(3/4): 409-416.
- [55] HILDRETH W. Volcanological perspectives on Long Valley, Mammoth Mountain, and Mono Craters: several contiguous but discrete systems[J]. Journal of Volcanology and Geothermal Research, 2004, 136(3/4): 169-198.
- [56] DEERING C D, BACHMANN O. Trace element indicators of crystal accumulation in silicic igneous rocks[J]. Earth and Planetary Science Letters, 2010, 297(1/2): 4-331.
- [57] BACHMANN O, BERGANTZ G W. Rhyolites and their source mushes across tectonic settings [J]. Journal of Petrology, 2008, 49(12): 2277-2285.
- [58] HOLNESS M B. Melt segregation from silicic crystal mushes: a critical appraisal of possible mechanisms and their microstructural record[J]. Contributions to Mineralogy and Petrology, 2018, 173(6): 48.
- [59] ANDERSON J R A T, SWIHART G H, ARTIOLI G, et al. Segregation vesicles, gas filter-pressing, and igneous differentiation[J]. The Journal of Geology, 1984, 92(1): 55-72.
- [60] SISSON T W, BACON C R. Gas-driven filter pressing in magmas[J]. Geology, 1999, 27(7): 613-616.
- [61] BROWN M, SOLAR G S. Shear-zone systems and melts: feedback relations and self-organization in orogenic belts[J]. Journal of Structural Geology, 1998, 20(2/3): 211-227.
- [62] ROSENBERG C L. Deformation of partially molten granite: a review and comparison of experimental and natural case studies[J]. International Journal of Earth Sciences, 2001, 90: 60-76.
- [63] NASIPURI P, BHATTACHARYA A, SATYANARAYANAN M. Localized pluton deformation and linked focused flow of low-volume fraction residual melt in deforming plagioclase cumulates[J]. Bulletin, 2011, 123(3/4): 669-680.
- [64] WEBBER J R, KLEPEIS K A, WEBB L E, et al. Deformation and magma transport in a crystallizing plutonic complex, Coastal Batholith, central Chile[J]. Geosphere, 2015, 11(5): 1401-1426.
- [65] ALLAN A S R, BARKER S J, MILLET M A, et al. A cascade of magmatic events during the assembly and eruption of a super-sized magma body[J]. Contrib Mineral Petrol, 2017, 172: 49
- [66] LIU X C, KOHN M J, WANG J M, et al. Formation of lithium-rich pegmatites via rapid crystallization and

- shearing-case study from the South Tibetan Detachment, Himalaya[J]. *Earth and Planetary Science Letters*, 2024, 629: 118598.
- [67] STEPANOV A, MAVROGENES J A, MEFFRE S, et al. The key role of mica during igneous concentration of tantalum[J]. *Contributions to Mineralogy and Petrology*, 2014, 167(6): 1-8.
- [68] SUN K K, CHEN B, DENG J. Ore genesis of the Zhuxi supergiant W-Cu skarn polymetallic deposit, South China: evidence from scheelite geochemistry[J]. *Ore Geology Reviews*, 2019, 107: 14-29.
- [69] DUFEK J, BACHMANN O. Quantum magmatism: magmatic compositional gaps generated by melt-crystal dynamics[J]. *Geology*, 2010, 38(8): 687-690.
- [70] PETRELLI M, OMARI K E, SPINA L, et al. Timescales of water accumulation in magmas and implications for short warning times of explosive eruptions[J]. *Nature Communications*, 2018, 9(1): 1-14.
- [71] ZHAO P L, YUAN S D, WILLIAMS-JONES A E, et al. Temporal separation of W and Sn mineralization by temperature-controlled incongruent melting of a single protolith: evidence from the Wangxianling area, Nanling region, South China[J]. *Economic Geology*, 2022, 117(3): 667-682.
- [72] IRBER W. The lanthanide tetrad effect and its correlation with K/Rb, Eu/Eu\*, Sr/Eu, Y/Ho, and Zr/Hf of evolving peraluminous granite suites[J]. *Geochimica et Cosmochimica Acta*, 1999, 63(3/4): 489-508.
- [73] LI J, HUANG X L, WEI G J, et al. Lithium isotope fractionation during magmatic differentiation and hydrothermal processes in rare-metal granites [J]. *Geochimica et Cosmochimica Acta*, 2018, 240: 64-79.
- [74] KAMENETSKY M B, SOBOLEV A V, KAMENETSKY V S, et al. Kimberlite melts rich in alkali chlorides and carbonates: a potent metasomatic agent in the mantle[J]. *Geology*, 2004, 32(10): 845-848.
- [75] DENG G X, JIANG D S, ZHANG R Q, et al. Barium isotopes reveal the role of deep magmatic fluids in magmatic-hydrothermal evolution and tin enrichment in granites[J]. *Earth and Planetary Science Letters*, 2022, 594: 1-10.
- [76] FREZZOTTI M L, GHEZZO C, STEFANINI B. The calabona intrusive complex (Sardinia, Italy): evidence for a porphyry copper system[J]. *Economic Geology*, 1992, 87(2): 425-436.
- [77] ZHANG D H, AUDÉTAT A. Magmatic-hydrothermal evolution of the barren Huangshan pluton, Anhui Province, China: a melt and fluid inclusion study[J]. *Economic Geology*, 2018, 113(4): 803-824.
- [78] WHITNEY J A. The origin of granite: the role and source of water in the evolution of granitic magmas[J]. *Geological Society of America Bulletin*, 1988, 100(12): 1886-1897.
- [79] WATERS L E, LANGE R A. Why aplites freeze and rhyolites erupt: controls on the accumulation and eruption of high-SiO<sub>2</sub> (eutectic) melts[J]. *Geology*, 2017, 45(11): 1019-1022.
- [80] 王德滋, 彭亚鸣, 袁朴. 福建魁岐花岗岩的岩石学和地球化学特征及成因探讨[J]. *地球化学*, 1985(3): 197-205.
- [81] 王德滋, 彭亚鸣, 袁朴. 福建魁岐花岗岩的岩石学和地球化学特征及成因探讨[J]. *地球化学*, 1985(3): 197-205.
- [82] WANG D Z, PENG Y M, YUAN P. Petrology, geochemistry and genesis of Kuiqi granite batholith[J]. *Geochimica*, 1985(3): 197-205.
- [83] 徐夕生. 华南花岗岩-火山岩成因研究的几个问题[J]. *高校地质学报*, 2008, 14(3): 283-294.
- [84] XU X S. Several problems worthy to be noticed in the research of granites and volcanic rocks in SE China[J]. *Geological Journal of China Universities*, 2008, 14(3): 283-294.
- [85] 黄小勇, 张辉, 唐勇, 等. 广西银屏富B花岗岩及其晶洞中电气石的化学组成特征以及对岩浆-热液演化的指示[J]. *矿物学报*, 2008, 28(1): 25-34.
- [86] HUANG X Y, ZHANG H, TANG Y, et al. Chemical composition of tourmalines from the B-rich granite and miarolitic cavities in Yinping, Guangxi and its implications for evolution of the magmatic hydrothermal system [J]. *Acta Mineralogica Sinica*, 2008, 28(1): 25-34.
- [87] LIU X H, LI B, LAI J Q, et al. Multistage in situ fractional crystallization of magma produced a unique rare metal enriched quartz-zinnwaldite-topaz rock[J]. *Ore Geology Reviews*, 2022, 151: 105203.
- [88] ZHOU J, JIANG Y H, XING G F, et al. Geochronology and petrogenesis of Cretaceous A-type granites from the NE Jiangnan Orogen, SE China[J]. *International Geology Review*, 2013, 55(11): 1359-1383.
- [89] XIANG L, ROMER R L, GLODNY J, et al. Li and B isotopic fractionation at the magmatic-hydrothermal transition of highly evolved granites[J]. *Lithos*, 2020, 376: 105753.
- [90] SONG S W, MAO J W, XIE G Q, et al. Petrogenesis of scheelite-bearing albite as an indicator for the formation of a world-class scheelite skarn deposit: a case study of the Zhuxi tungsten deposit[J]. *Economic Ge-*

- ology, 2021, 116(1): 91-121.
- [87] WATERS L E, LANGE R A. Why aplites freeze and rhyolites erupt: controls on the accumulation and eruption of high-SiO<sub>2</sub> (eutectic) melts[J]. *Geology*, 2017, 45(11): 1019-1022.
- [88] MÜLLER A, SELTMANN R. The genetic significance of snowball quartz in high fractionated tin granites of the Krušne Hory/Erzgebirge[J]. *Mineral deposits*, 1999(1): 409-412.
- [89] YANG J, SIEBERT C, BARLING J, et al. Absence of molybdenum isotope fractionation during magmatic differentiation at Hekla volcano, Iceland [J]. *Geochimica et Cosmochimica Acta*, 2015, 162: 126-136.
- [90] 李福春, 朱金初, 金章东, 等. 钠长石花岗岩中雪球结构形成机理的研究[J]. *岩石矿物学杂志*, 2000, 19(1): 27-35.
- LI F C, ZHU J C, JIN Z D, et al. Formation mechanism of snowball texture in albite granite[J]. *Acta Petrologica et Mineralogica*, 2000, 19(1): 27-35.
- [91] 杨飞, 武广, 陈公正, 等. 维拉斯托稀有金属-锡多金属矿床铌铁矿族矿物特征及其对岩浆-热液演化的指示[J]. *矿床地质*, 2023, 42(3): 463-480.
- YANG F, WU G, CHEN G Z, et al. Compositional and textural variations of columbite group minerals from Weilasituo rare metal-tin polymetallic deposit: implications for tracing magmatic-hydrothermal evolution[J]. *Mineral Deposits*, 2023, 42(3): 463-480.
- [92] 邹海波, 徐洪武, 周新民. 钽花岗岩中雪球结构的成因研究[J]. *科学通报*, 1991, 36(16): 1245-1247.
- ZOU H B, XU H W, ZHOU X M. A study of the genesis of snowball structures in tantalum granites[J]. *Chinese Science Bulletin*, 1991, 36(16): 1245-1247.
- [93] WU M Q, SAMSON I M, ZHANG D H. Textural features and chemical evolution in Ta-Nb oxides: implications for deuterium rare-metal mineralization in the Yichun granite-marginal pegmatite, Southeastern China[J]. *Economic Geology*, 2018, 113(4): 937-960.
- [94] WANG D Z, LIU J J, CARRANZA E J M, et al. Formation and evolution of snowball quartz phenocrysts in the Dongping porphyritic granite, Hebei Province, China: insights from fluid inclusions, cathodoluminescence, trace elements, and crystal size distribution study[J]. *Lithos*, 2019, 340: 239-254.
- [95] LU T Y, HE Z Y, KLEMD R. Identifying crystal accumulation and melt extraction during formation of high-silica granite [J]. *Geology*, 2022, 50 (2): 216-221.
- [96] POLLARD P J. The Yichun Ta-Sn-Li deposit, South China: evidence for extreme chemical fractionation in F-Li-P-rich magma[J]. *Economic Geology*, 2021, 116(2): 453-469.
- [97] SHANNON J R, WALKER B M, CARTEN R B, et al. Unidirectional solidification textures and their significance in determining relative ages of intrusions at the Henderson Mine, Colorado[J]. *Geology*, 1982, 10(6): 293-297.
- [98] YANG Z M, LU Y J, HOU Z Q, et al. High-Mg diorite from Qulong in southern Tibet: implications for the genesis of adakite-like intrusions and associated porphyry Cu deposits in collisional orogens[J]. *Journal of Petrology*, 2015, 56(2): 227-254.
- [99] HÖNIG S, LEICHMANN J, NOVAK M. Unidirectional solidification textures and garnet layering in Y-enriched garnet-bearing aplite-pegmatites in the Cadomian Brno Batholith, Czech Republic[J]. *Journal of Geosciences*, 2010, 55(2): 113-129.
- [100] SILLITOE R H. Porphyry copper systems[J]. *Economic Geology*, 2010, 105: 3-41.
- [101] MÜLLER A, KIRWIN D, SELTMANN R. Textural characterization of unidirectional solidification textures related to Cu-Au deposits and their implication for metallogenesis and exploration[J]. *Mineralium Deposita*, 2023, 1-25.
- [102] PEPPARD D F, MASON G W, LEWEY S. A tetrad effect in the liquid-liquid extraction ordering of lanthanides (III) [J]. *Journal of Inorganic and Nuclear Chemistry*, 1969, 31(7): 2271-2272.
- [103] MASUDA A, IKEUCHI Y. Lanthanide tetrad effect observed in marine environment [J]. *Geochemical Journal*, 1979, 13(1): 19-22.
- [104] HIDAKA H, HOLLIGER P, SHIMIZU H, et al. Lanthanide tetrad effect observed in the Oklo and ordinary uraninites and its implication for their forming processes[J]. *Geochemical Journal*, 1992, 26 (6): 337-346.
- [105] AKAGI T, SHABANI M B, MASUDA A. Lanthanide tetrad effect in kimuraite [CaY<sub>2</sub>(CO<sub>3</sub>)<sub>4</sub> • 6H<sub>2</sub>O]: implication for a new geochemical index[J]. *Geochimica et Cosmochimica Acta*, 1993, 57 (12): 2899-2905.
- [106] TAKAHASHI T, SUTHERLAND S C, SWEENEY C, et al. Global sea-air CO<sub>2</sub> flux based on climatological surface ocean pCO<sub>2</sub>, and seasonal biological and

- temperature effects[J]. Deep Sea Research Part II: Topical Studies in Oceanography, 2002, 49(9/10): 1601-1622.
- [107] 赵振华. 花岗岩中发现稀土元素四重分布效应的初步报道[J]. 地质地球化学, 1988(1): 71-72.  
ZHAO Z H. A preliminary report on the discovery of the quadruple distribution effect of rare earth elements in granites[J]. Geological Geochemistry, 1988(1): 71-72.
- [108] 赵振华, 包志伟, 乔玉楼. 一种特殊的“M”与“W”复合型稀土元素四分组效应: 以水泉沟碱性正长岩为例[J]. 科学通报, 2010, 55(15): 1474-1488.  
ZHAO Z H, BAO Z W, QIAO Y L. A peculiar composite M-and W-type REE tetrad effect: evidence from the Shuiquangou alkaline syenite complex, Hebei Province, China[J]. Chinese Science Bulletin, 2010, 55(15): 1474-1488.
- [109] SUN S S, McDONOUGH W F. Chemical and isotopic systematics of oceanic basalts: implications for mantle composition and processes[J]. Geological Society, 1989, 42(1): 313-345.
- [110] MCLENNAN S M. Rare earth element geochemistry and the “tetrad” effect[J]. Geochimica et Cosmochimica Acta, 1994, 58(9): 2025-2033.
- [111] PAN Y W, BREAKS F W. Rare-earth elements in fluorapatite, Separation Lake area, Ontario: evidence for S-type granite-rare-element pegmatite linkage[J]. The Canadian Mineralogist, 1997, 35(3): 659-671.
- [112] DUC-TIN Q, KEPPLER H. Monazite and xenotime solubility in granitic melts and the origin of the lanthanide tetrad effect[J]. Contributions to Mineralogy and Petrology, 2015, 169: 1-26.
- [113] 赵振华, 熊小林, 韩小东. 花岗岩稀土元素四分组效应形成机理探讨——以千里山和巴尔哲花岗岩为例[J]. 中国科学(D辑), 1999, 29(4): 331-338.  
ZHAO Z H, XIONG X L, HAN X D. Exploration of the formation mechanism of the four-grouping effect of rare earth elements in granite—taking Qianli Mountain and Balzhe granite as an example [J]. Science in China(Series D), 1999, 29(4): 331-338.
- [114] MONECKE T, KEMPE U, GÖTZE J. Genetic significance of the trace element content in metamorphic and hydrothermal quartz: a reconnaissance study[J]. Earth and Planetary Science Letters, 2002, 202(3/4): 709-724.
- [115] BARTH M C, RASCH P J, KIEHL J T, et al. Sulfur chemistry in the national center for atmospheric research community climate model: description, evaluation, features, and sensitivity to aqueous chemistry [J]. Journal of Geophysical Research, 2000, 105(D1): 1387-1415.
- [116] 谭东波, 李东永, 肖益林. “孪生元素”铌-钽的地化特性研究进展[J]. 地球科学, 2018, 43(1): 317-332.  
TAN D B, LI D Y, XIAO Y L. Geochemical characteristics of niobium and tantalum: a review of twin elements[J]. Earth Science, 2018, 43(1): 317-332.
- [117] RAIMBAULT L, CUNNEY M, AZENCOTT C, et al. Geochemical evidence for a multistage magmatic genesis of Ta-Sn-Li mineralization in the granite at Beauvoir, French Massif Central[J]. Economic Geology, 1995, 90(3): 548-576.
- [118] LINNEN R L, LICHTERVELDE M V, ČERNÝ P. Granitic pegmatites as sources of strategic metals[J]. Elements, 2012, 8(4): 275-280.
- [119] STEPANOV A S, HERMANN J. Fractionation of Nb and Ta by biotite and phengite: implications for the “missing Nb paradox”[J]. Geology, 2013, 41(3): 303-306.
- [120] LINNEN R L, KEPPLER H. Columbite solubility in granitic melts: consequences for the enrichment and fractionation of Nb and Ta in the Earth’s crust[J]. Contributions to Mineralogy and Petrology, 1997, 128: 213-227.
- [121] LINNEN R L. The solubility of Nb-Ta-Zr-Hf-W in granitic melts with Li and Li + F: constraints for mineralization in rare metal granites and pegmatites [J]. Economic Geology, 1998, 93(7): 1013-1025.
- [122] BARTELS A, HOLTZ F, LINNEN R L. Solubility of manganotantalite and manganocolumbite in pegmatitic melts[J]. American Mineralogist, 2010, 95(4): 537-544.
- [123] CHEVYCHELOV V Y, BORODULIN G P, ZARISKY G P. Solubility of columbite,  $(\text{Mn}, \text{Fe})(\text{Nb}, \text{Ta})_2\text{O}_6$ , in granitoid and alkaline melts at 650-850 °C and 30-400 MPa: an experimental investigation[J]. Geochemistry International, 2010, 48: 456-464.
- [124] GAO M D, XIONG X L, HUANG F F, et al. Key factors controlling biotite-silicate melt Nb and Ta partitioning: implications for Nb-Ta enrichment and fractionation in granites[J]. Journal of Geophysical Research: Solid Earth, 2023, 128(7): e2022JB025889.
- [125] VIGNERESSE J L, BARBEY P, CUNNEY M. Rheological transitions during partial melting and crystalli-

- zation with application to felsic magma segregation and transfer[J]. *Journal of Petrology*, 1996, 37(6): 1579-1600.
- [126] LINNEN R L, CUNNEY M. Granite-related rare-element deposits and experimental constraints on Ta-Nb-W-Sn-Zr-Hf mineralization [M] // LINNEN R L, SAMSON I M. Rare-element geochemistry and mineral deposits. Canada: Geological Association of Canada short course, 2005.
- [127] ZARAISKY G P, KORZHINSKAYA V, KOTOVA N. Experimental studies of  $Ta_2O_5$  and columbite-tantalite solubility in fluoride solutions from 300 to 550°C and 50 to 100 MPa[J]. *Mineralogy and Petrology*, 2010, 99(3/4): 287-300.
- [128] DOSTAL J, CHATTERJEE A K. Contrasting behaviour of Nb/Ta and Zr/Hf ratios in a peraluminous granitic pluton (Nova Scotia, Canada)[J]. *Chemical Geology*, 2000, 163(1/4): 207-218.
- [129] NI P, WANG X D, WANG G G, et al. An infrared microthermometric study of fluid inclusions in coexisting quartz and wolframite from Late Mesozoic tungsten deposits in the Gannan metallogenic belt, South China [J]. *Ore Geology Reviews*, 2015, 65: 1062-1077.
- [130] 吴元保, 郑永飞. 锆石成因矿物学研究及其对 U-Pb 年龄解释的制约[J]. *科学通报*, 2004, 49(16): 1589-1604.
- WU Y B, ZHENG Y F. Mineralogical study of zircon genesis and its constraints on U-Pb age interpretation[J]. *Chinese Science Bulletin*, 2004, 49(16): 1589-1604.
- [131] CHAKOUMAKOS B C, MURAKAMI T, LUMPKIN G R, et al. Alpha-decay-induced fracturing in zircon: the transition from the crystalline to the metamict state[J]. *Science*, 1987, 236(4808): 1556-1559.
- [132] EWING R C, WANG L M, WEBER W J. Amorphization of complex ceramics by heavy-particle irradiations [J]. *MRS Online Proceedings Library (OPL)*, 1994, 373: 347.
- [133] WILLIAMS I S, HERGT JM. U-Pb dating of Tasmanian dolerites: a cautionary tale of SHRIMP analysis of high-U zircon[C]// WOODHEAD J D, HERGT J M, NOBLE N P. Beyond 2000: New frontiers in isotope geoscience. Lorne, 2000: 185-188.
- [134] WHITE L T, IRELAND T R. High-uranium matrix effect in zircon and its implications for SHRIMP U-Pb age determinations [J]. *Chemical Geology*, 2012, 306/307: 78-91.
- [135] SILVER L T, DEUTSCH S. Uranium-lead isotopic variations in zircons: a case study[J]. *The Journal of Geology*, 1963, 71(6): 721-758.
- [136] SHANNON R D. Revised effective ionic radii and systematic studies of interatomic distances in Halides and Chalcogenides[J]. *Acta Crystallographica Section A*, 1976, 32(5): 751-767.
- [137] YANG W B, NIU H C, SHAN Q, et al. Geochemistry of magmatic and hydrothermal zircon from the highly evolved Baerzhe alkaline granite: implications for Zr-REE-Nb mineralization[J]. *Mineralium Deposita*, 2014, 49: 451-470.
- [138] LI H, HU X J, ELATIKPO S M, et al. Zircon as a pathfinder for ore exploration [J]. *Journal of Geochemical Exploration*, 2023, 249: 107216.
- [139] REED R, LEMAK D J, MERO N P. Total quality management and sustainable competitive advantage [J]. *Journal of Quality Management*, 2000, 5(1): 5-26.
- [140] HOSKIN P W O. Trace-element composition of hydrothermal zircon and the alteration of Hadean zircon from the Jack Hills, Australia[J]. *Geochimica et Cosmochimica Acta*, 2005, 69(3): 637-648.
- [141] JIANG W C, LI H, EVANS N J, et al. Zircon records multiple magmatic-hydrothermal processes at the giant Shizhuoyuan W-Sn-Mo-Bi polymetallic deposit, South China[J]. *Ore Geology Reviews*, 2019, 115: 103160.
- [142] HERMANN J. Allanite: thorium and light rare earth element carrier in subducted crust[J]. *Chemical Geology*, 2002, 192(3/4): 289-306.
- [143] NOZHKIN A D, TURKINA O M. Radiogeochimistry of the charnockite-granulite complex, Sharyzhalgay Window, Siberian Platform[J]. *Geochemistry International*, 1995, 32(2): 62-78.
- [144] 箕昊翔, 王志强, 袁峰, 等. 皖南伏岭岩体钾长石地球化学特征及其成因意义[J]. *合肥工业大学学报(自然科学版)*, 2024, 待刊.
- DA H X, WANG Z Q, YUAN F, et al. Geochemical characteristics of K-feldspar from the Fuling pluton in southern Anhui and its genetic significance [J]. *Journal of Hefei University of Technology (Natural Science)*, 2024, accepted.
- [145] ZAJACZ Z, HALTER W E, PETTKE T, et al. Determination of fluid/melt partition coefficients by LA-ICPMS analysis of co-existing fluid and silicate melt inclusions: controls on element partitioning [J].

- Geochimica et Cosmochimica Acta, 2008, 72(8): 2169-2197.
- [146] 黄方. 高温下非传统稳定同位素分馏[J]. 岩石学报, 2011, 27(2): 365-382.  
HUANG F. Non-traditional stable isotope fractionation at high temperatures[J]. *Acta Petrologica Sinica*, 2011, 27(2): 365-382.
- [147] 朱祥坤, 孙剑, 王跃. 岩浆过程中铁同位素的地球化学行为[J]. 地球科学与环境学报, 2016, 38(1): 1-10.  
ZHU X K, SUN J, WANG Y. Fe isotope geochemistry of magmatic system[J]. *Journal of Earth Sciences and Environment*, 2016, 38(1): 1-10.
- [148] 王昆, 李伟强, 李石磊. 钾稳定同位素研究综述[J]. 地学前缘, 2020, 27(3): 104-122.  
WANG K, LI W Q, LI S L. Stable potassium isotope geochemistry and cosmochemistry[J]. *Earth Science Frontiers*, 2020, 27(3): 104-122.
- [149] 陆一敢, 肖益林, 王洋洋, 等. Li 同位素在矿床学中的应用: 现状与展望 [J]. 地球科学, 2021, 46(12): 4346-4365.  
LU Y G, XIAO Y L, WANG Y Y, et al. Exploration of Li isotope in application of ore deposits[J]. *Earth Science*, 2021, 46(12): 4346-4365.
- [150] 顾海欧, 刘倩, 孙贺. 钾同位素的高精度分析及深部过程的示踪应用[J]. 地质学报, 2022, 96(12): 4331-4339.  
GU H O, LIU Q, SUN H. High precision potassium isotope analysis and its application in tracing deep earth processes[J]. *Acta Geologica Sinica*, 2022, 96(12): 4331-4339.
- [151] TOMASCAK P B, TERA F, HELZ R T, et al. The absence of lithium isotope fractionation during basalt differentiation: new measurements by multicollector sector ICP-MS [J]. *Geochimica et Cosmochimica Acta*, 1999, 63(6): 907-910.
- [152] CHAN L H, FREY F A. Lithium isotope geochemistry of the Hawaiian plume: results from the Hawaii scientific drilling project and Koolau volcano[J]. *Geochemistry, Geophysics, Geosystems*, 2003, 4(3): 1-20.
- [153] JEFFCOATE A B, ELLIOTT T, KASEMANN S A, et al. Li isotope fractionation in peridotites and mafic melts[J]. *Geochimica et Cosmochimica Acta*, 2007, 71(1): 202-218.
- [154] TENG F Z, MCDONOUGH W F, RUDNICK R L, et al. Lithium isotopic systematics of granites and pegmatites from the Black Hills, South Dakota[J]. *American Mineralogist*, 2006, 91(10): 1488-1498.
- [155] 何永胜, 胡东平, 朱传卫. 地球科学中铁同位素研究进展[J]. 地学前缘, 2015, 22(5): 54-71.  
HE Y S, HU D P, ZHU C W. Progress of iron isotope geochemistry in geoscience[J]. *Earth Science Frontiers*, 2015, 22(5): 54-71.
- [156] SEITZ H M, WOODLAND A B. The distribution of lithium in peridotitic and pyroxenitic mantle lithologies—an indicator of magmatic and metasomatic processes[J]. *Chemical Geology*, 2000, 166(1/2): 47-64.
- [157] MCDONOUGH W F, SUN S S. The composition of the Earth[J]. *Chemical Geology*, 1995, 120(3/4): 223-253.
- [158] SALTERS V J M, STRACKE A. Composition of the depleted mantle[J]. *Geochemistry, Geophysics, Geosystems*, 2004, 5(5): 1-27.
- [159] TENG F Z, RUDNICK R L, MCDONOUGH W F, et al. Lithium isotopic composition and concentration of the deep continental crust[J]. *Chemical Geology*, 2008, 255(1/2): 47-59.
- [160] FOUSTOUKOS D I, JAMES R H, BERNDT M E, et al. Lithium isotopic systematics of hydrothermal vent fluids at the Main Endeavour field, Northern Juan de Fuca Ridge[J]. *Chemical Geology*, 2004, 212(1/2): 17-26.
- [161] 孙贺. 熔体包裹体和 Li 同位素在地球科学研究中的应用[D]. 合肥: 中国科学技术大学, 2014: 1-221.  
SUN H. Application of melt inclusions and Li isotope in earth sciences[D]. Hefei: University of Science and Technology of China, 2014: 1-221.
- [162] TOMASCAK P B, MAGNA T, DOHMHEN R. Advances in lithium isotope geochemistry[M]. Switzerland: Springer International Publishing, 2016: 1-195.
- [163] TANG Y J, ZHANG H F, NAKAMURA E, et al. Lithium isotopic systematics of peridotite xenoliths from Hannuoba, North China Craton: implications for melt-rock interaction in the considerably thinned lithospheric mantle[J]. *Geochimica et Cosmochimica Acta*, 2007, 71(17): 4327-4341.
- [164] TOMASCAK P B, LANGMUIR C H, LE ROUX P J, et al. Lithium isotopes in global mid-ocean ridge basalts[J]. *Geochimica et Cosmochimica Acta*, 2008, 72(6): 1626-1637.
- [165] TENG F Z, MCDONOUGH W F, RUDNICK R L, et al. Lithium isotopic composition and concentration

- of the upper continental crust[J]. *Geochimica et Cosmochimica Acta*, 2004, 68(20): 4167-4178.
- [166] TENG F Z, RUDNICK R L, MCDONOUGH W F, et al. Lithium isotopic systematics of A-type granites and their mafic enclaves: further constraints on the Li isotopic composition of the continental crust [J]. *Chemical Geology*, 2009, 262(3/4): 370-379.
- [167] YANG J H, CHEN H, ZHOU M F, et al. Lithium isotope fractionation during intensive felsic magmatic differentiation[J]. *Geochemistry, Geophysics, Geosystems*, 2023, 24(4): 1-20.
- [168] SUN H, GAO Y J, XIAO Y L, et al. Lithium isotope fractionation during incongruent melting: constraints from post-collisional leucogranite and residual enclaves from Bengbu Uplift, China [J]. *Chemical Geology*, 2016, 439: 71-82.
- [169] VLASTÉLIC I, STAUDACHER T, BACHÈLERY P, et al. Lithium isotope fractionation during magma degassing: constraints from silicic differentiates and natural gas condensates from Piton de la Fournaise volcano (Réunion Island) [J]. *Chemical Geology*, 2011, 284(1/2): 26-34.
- [170] FAN J J, TANG G J, WEI G J, et al. Lithium isotope fractionation during fluid exsolution: implications for Li mineralization of the Bailongshan pegmatites in the West Kunlun, NW Tibet. [J]. *Lithos*, 2020, 352/353: 1-17.
- [171] ZHANG H J, TIAN S H, WANG D H, et al. Lithium isotope behavior during magmatic differentiation and fluid exsolution in the Jiajika granite-pegmatite deposit, Sichuan, China[J]. *Ore Geology Reviews*, 2021, 134: 1-12.
- [172] ELLIS B S, NEUKAMPF J, BACHMANN O, et al. Biotite as a recorder of an exsolved Li-rich volatile phase in upper-crustal silicic magma reservoirs [J]. *Geology*, 2022, 50(4): 481-485.
- [173] NEUKAMPF J, ELLIS B S, MAGNA T, et al. Partitioning and isotopic fractionation of lithium in mineral phases of hot, dry rhyolites: the case of the Mesa Falls Tuff, Yellowstone[J]. *Chemical Geology*, 2019, 506: 175-186.
- [174] NEUKAMPF J, LAURENT O, TOLLAN P, et al. Degassing from magma reservoir to eruption in silicic systems: the Li elemental and isotopic record from rhyolitic melt inclusions and host quartz in a Yellowstone rhyolite[J]. *Geochimica et Cosmochimica Acta*, 2022, 326: 56-76.
- [175] LI X F, WANG Z Q, CHEN B, et al. Lithium isotope fractionation in highly evolved granites and associated magmatic-hydrothermal process: the case of the Xintianling granites in the Nanling Range, South China[J]. *International Geology Review*, 2024: 1-23. <http://doi.org/10.1080/00206814.2021.2309490>.
- [176] SUN S S, MCDONOUGH W F. Chemical and isotopic systematics of oceanic basalts: implications for mantle composition and processes[J]. *Geological Society*, 1989, 42(1): 313-345.
- [177] RUDNICK R L, GAO S. Composition of the continental crust[J]. *Treatise on Geochemistry*, 2003(3): 1-64.
- [178] KELLER C B, SCHÖENE B, BARBONI M, et al. Volcanic-plutonic parity and the differentiation of the continental crust[J]. *Nature*, 2015, 523: 301-307.
- [179] KESSEL R, SCHMIDT M W, ULMER P, et al. Trace element signature of subduction-zone fluids, melts and supercritical liquids at 120-180km depth [J]. *Nature*, 2005, 437(7059): 724-727.
- [180] MORRIS J D, RYAN J G. Subduction zone processes and implications for changing composition of the upper and lower mantle [J]. *Treatise on Geochemistry*, 2003, 2: 451-467.
- [181] EUGSTER O, TERA F, WASSERBURG G J. Isotopic analyses of barium in meteorites and in terrestrial samples[J]. *Journal of Geophysical Research*, 1969, 74(15): 3897-3908.
- [182] NIELSEN S G, HORNER T J, PRYER H V, et al. Barium isotope evidence for pervasive sediment recycling in the upper mantle [J]. *Science Advances*, 2018, 4(7): 1-9.
- [183] NAN X Y, YU H M, KANG J T, et al. Re-visiting barium isotope compositions of mid-ocean ridge basalts and the implications[J]. *Journal of University of Science and Technology of China*, 2022, 52(3): 1-7.
- [184] NAN X Y, YU H M, RUDNICK R L, et al. Barium isotopic composition of the upper continental crust[J]. *Geochimica et Cosmochimica Acta*, 2018, 233: 33-49.
- [185] HUANG F, BAI R X, DENG G X, et al. Barium isotope evidence for the role of magmatic fluids in the origin of Himalayan leucogranites[J]. *Science Bulletin*, 2021, 66(22): 2329-2336.
- [186] DENG G X, KANG J T, NAN X Y, et al. Barium isotope evidence for crystal-melt separation in granitic magma reservoirs[J]. *Geochimica et Cosmochimica*

- Acta, 2021, 292: 115-129.
- [187] BULLEN T, CHADWICK O. Ca, Sr and Ba stable isotopes reveal the fate of soil nutrients along a tropical climosequence in Hawaii [J]. *Chemical Geology*, 2016, 422: 25-45.
- [188] GUO H, LI W Y, NAN X, et al. Experimental evidence for light ba isotopes favouring aqueous fluids over silicate melts[J]. *Geochemical Perspectives Letters*, 2020, 16: 6-11.
- [189] WANG W Z, WU Z Q, HUANG F. Equilibrium barium isotope fractionation between minerals and aqueous solution from first-principles calculations[J]. *Geochimica et Cosmochimica Acta*, 2021, 292: 64-77.
- [190] JOHNSON C M, BEARD B L, KLEIN C, et al. Iron isotopes constrain biologic and abiologic processes in banded iron formation genesis[J]. *Geochimica et Cosmochimica Acta*, 2008, 72(1): 151-169.
- [191] DAUPHAS N, CRADDOCK P R, ASIMOW P D, et al. Iron isotopes may reveal the redox conditions of mantle melting from Archean to Present[J]. *Earth and Planetary Science Letters*, 2009, 288 (1/2): 255-267.
- [192] WEYER S, IONOV D A. Partial melting and melt percolation in the mantle: the message from Fe isotopes[J]. *Earth and Planetary Science Letters*, 2007, 259(1/2): 119-133.
- [193] TENG F Z, DAUPHAS N, HUANG S C, et al. Iron isotopic systematics of oceanic basalts[J]. *Geochimica et Cosmochimica Acta*, 2013, 107: 12-26.
- [194] DU D H, WANG X L, YANG T, et al. Origin of heavy Fe isotope compositions in high-silica igneous rocks: a rhyolite perspective[J]. *Geochimica et Cosmochimica Acta*, 2017, 218: 58-72.
- [195] FODEN J, SOSSI P A, WAWRYK C M, et al. Fe isotopes and the contrasting petrogenesis of A-, I-and S-type granite[J]. *Lithos*, 2015, 212: 32-44.
- [196] XIA Y, LI S Q, HUANG F. Iron and Zinc isotope fractionation during magmatism in the continental crust: evidence from bimodal volcanic rocks from Hailar basin, NE China[J]. *Geochimica et Cosmochimica Acta*, 2017, 213: 35-46.
- [197] MA H Z, CHEN Y X, ZHOU K, et al. The effect of crystal fractionation on the geochemical composition of syn-exhumation magmas: implication for the formation of high  $\delta^{56}\text{Fe}$  granites in collisional orogens [J]. *Geochimica et Cosmochimica Acta*, 2022, 332: 156-185.
- [198] SOSSI P A, FODEN J D, HALVERSON G P. Redox-controlled iron isotope fractionation during magmatic differentiation: an example from the Red Hill intrusion, S. Tasmania[J]. *Contributions to Mineralogy and Petrology*, 2012, 164(5): 757-772.
- [199] HEIMANN A, BEARD B L, JOHNSON C M. The role of volatile exsolution and sub-solidus fluid/rock interactions in producing high  $^{56}\text{Fe}/^{54}\text{Fe}$  ratios in siliceous igneous rocks[J]. *Geochimica et Cosmochimica Acta*, 2008, 72(17): 4379-4396.
- [200] AUDÉTAT A, PETTKE T. The magmatic-hydrothermal evolution of two barren granites: a melt and fluid inclusion study of the Rito del Medio and Canada Pinabete plutons in northern New Mexico (USA)[J]. *Geochimica et Cosmochimica Acta*, 2003, 67 (1): 97-121.
- [201] TELUS M, DAUPHAS N, MOYNIER F, et al. Iron, zinc, magnesium and uranium isotopic fractionation during continental crust differentiation: the tale from migmatites, granitoids, and pegmatites[J]. *Geochimica et Cosmochimica Acta*, 2012, 97: 247-265.
- [202] POITRASSON F, FREYDIER R. Heavy iron isotope composition of granites determined by high resolution MC-ICP-MS[J]. *Chemical Geology*, 2005, 222(1/2): 132-147.
- [203] FUJII T, MOYNIER F, BLICHERT-TOFT J, et al. Density functional theory estimation of isotope fractionation of Fe, Ni, Cu, and Zn among species relevant to geochemical and biological environments [J]. *Geochimica et Cosmochimica Acta*, 2014, 140: 553-576.
- [204] WANG Y, ZHU X K, CHENG Y B. Fe isotope behaviours during sulfide-dominated skarn-type mineralisation[J]. *Journal of Asian Earth Sciences*, 2015, 103: 374-392.
- [205] THOMAS R, FÖRSTER H J, HEINRICH W. The behaviour of boron in a peraluminous granite-pegmatite system and associated hydrothermal solutions: a melt and fluid-inclusion study[J]. *Contributions to Mineralogy and Petrology*, 2003, 144 (4): 457-472.
- [206] HULSBOSCH N, HERTOGEN J, DEWAELÉ S, et al. Alkali metal and rare earth element evolution of rock-forming minerals from the Gatumba area pegmatites (Rwanda): quantitative assessment of crystal-melt fractionation in the regional zonation of pegmatite groups[J]. *Geochimica et Cosmochimica Acta*, 2014, 132: 349-374.

- [207] LONDON D. A Rayleigh model of cesium fractionation in granite-pegmatite systems [J]. American Mineralogist, 2022, 107(1): 82-91.
- [208] 朱金初, 王汝成, 陆建军, 等. 湘南癞子岭花岗岩体分异演化和成岩成矿[J]. 高校地质学报, 2011, 17(3): 381-392.
- ZHU J C, WANG R C, LU J J, et al. Fractionation, evolution, petrogenesis and mineralization of Laiziling granite pluton, southern Hunan Province [J]. Geological Journal of China Universities, 2011, 17(3): 381-392.
- [209] SCHMIDT C, ROMER R L, WOHLGEMUTH-UEBERWASSER C C, et al. Partitioning of Sn and W between granitic melt and aqueous fluid[J]. Ore Geology Reviews, 2020, 117: 103263.
- [210] QIU Y, WANG X, LU J, et al. Insitu observations of tungsten speciation and partitioning behavior during fluid exsolution from granitic melt [J]. Science Bulletin, 2022, 67(22): 2358-2368.
- [211] WEBSTER J D, HOLLOWAY J R, HERVIG R L. Partitioning of lithophile trace elements between  $H_2O$  and  $H_2O+CO_2$  fluids and topaz rhyolite melt[J]. Economic Geology, 1989, 84(1): 116-134.
- [212] BRENAN J M, SHAW H F, PHINNEY D L, et al. Rutile-aqueous fluid partitioning of Nb, Ta, Hf, Zr, U and Th: implications for high field strength element depletions in island-arc basalts[J]. Earth and Planetary Science Letters, 1994, 128(3/4): 327-339.

## Identification and significance of fluid exsolution in high silica granite

WANG Zhiqiang<sup>1,2</sup>, ZHOU Meijuan<sup>1,2</sup>, LI Xunfei<sup>1,2</sup>, DA Haoxiang<sup>1,2</sup>

(1. Ore Deposit and Exploration Centre (ODEC), School of Resources and Environmental Engineering,

Hefei University of Technology, Hefei 230009, Anhui, China;

2. Anhui Province Engineering Research Center for Mineral Resources and Mine Environments,

Hefei 230009, Anhui, China)

**Abstract:** High silica granite is characterized with low content of dark minerals, abundant  $SiO_2$ , Rb, poor MgO, FeO, Sr, Ba, and enrichment of rare metal elements. Research on it is crucial to understand the petrogenesis of granite, the enrichment of rare metal elements and mineralization process. The petrographic and geochemical characteristics indicate that it has undergone a high degree of differentiation evolution. Volatile components such as  $H_2O$ , as incompatible components, are gradually enriched and eventually saturated in the residual melt, resulting in inevitable fluid dissolution in high silica granitic melts, but how to identify it is difficult. This paper summarizes the evidence and indicators for fluid exsolution in high silica granite from the perspectives of petrography, whole-rock geochemistry, mineralogy, and metal stable isotopes (Li, Ba, Fe). The appearance of miarolitic structure, snowball texture and unidirectional solidification texture are important petrographic signs of fluid exsolution. In terms of whole-rock geochemistry, extremely low Nb/Ta values (<5), Zr/Hf values and the tetrad effect of rare earth elements are effective identifiers of fluid-melt interaction. In mineralogy, metamictization and LREE enrichment of zircon and high Pb content in K-feldspar indicate the involvement of hydrothermal fluids. Compared to common granite, high silica granite is usually enriched with heavy Li, light Ba, and heavy Fe isotopes. Fluid-melt interaction is probably the major factor in isotope fractionation of high silica granite. However, some geochemical evidence remains controversial, so we recommend to use together the various lines of evidence. After the two-stage enrichment process of magma evolution and fluid exsolution, rare metal elements can be extremely enriched in the exsolved fluid and then mineralized.

**Key words:** high silica granite; fluid exsolution; magmatic-hydrothermal transition; metal stable isotopes; rare-metal mineralization